Quark–Antiquark States and their Radiative Decays in terms of the Spectral Integral Equation. Light–Quark States, Charmonia, Bottomonia.

V.V. Anisovich, L.G. Dakhno, M.A. Matveev, V.A. Nikonov, A.V. Sarantsev

Introduction

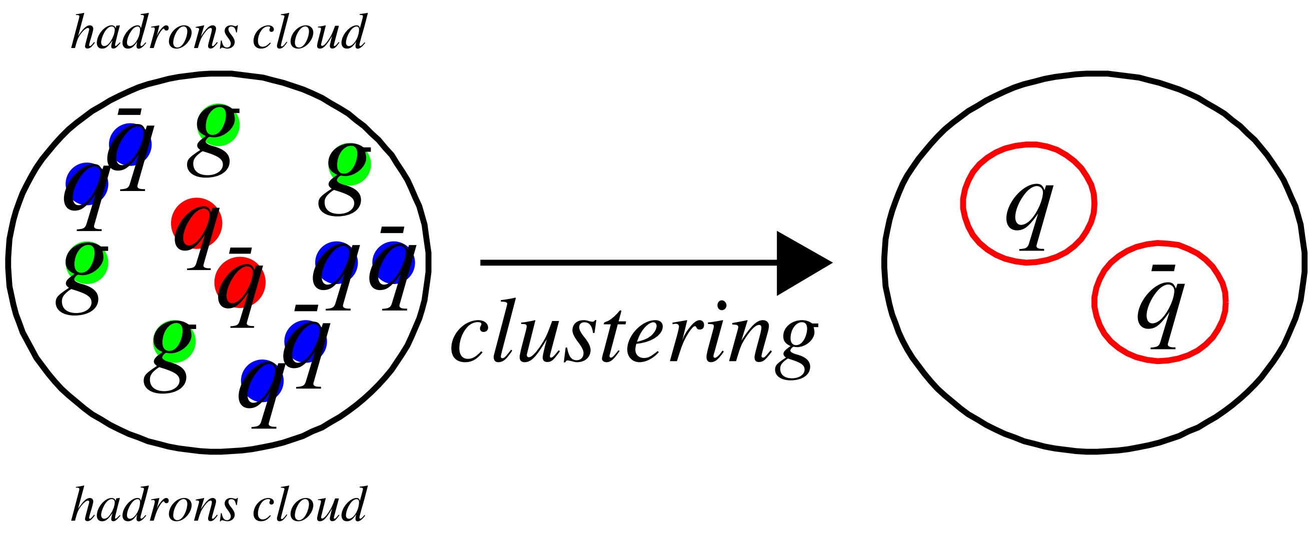

Quark-gluon matter:

$q\bar{q}$ – valence quarks

$q\bar{q}$ – sea quarks

g – gluons

hadron's cloud (pions)

$q\bar{q}$ – constituent quarks

confinment wall

In recent decade, considerable progress has been achieved in meson and baryon physics:

a)A large number of meson states has been discovered (in the main, in the mass interval $1500 \lesssim M \lesssim 2400$ MeV)

b) Wonderful fact is that the majority of mesons lie on linear trajectories in the (n, M^2)- and (J, M^2)-planes.

c) As a whole, mesons can be treated as quark–antiquark states.

d) Baryon states also belong to linear trajectories.

Progress: 4–5 resonances on one trajectory!

Interaction forces between quarks?

(i)Bethe–Salpeter Equation

(ii) Spectral Integral Equation — dispersion relation approach, with the following advantages:

the right-hand cut is strictly controlled as well as the resonance content,

dispersion approach allows one to reconstruct the left-hand cut.

Constituent quarks and effective gluons:

$u, d \sim 300 - 400$ MeV ($m_{u,d}^{QCD} =$ 4,7 MeV)

$s \sim 500$ MeV ($m_s^{QCD} \sim$ 80–150 MeV)

$c \sim 1200 - 1500$ MeV ($m_c^{QCD} \sim$ 1.0–1.4 GeV)

$b \sim 4500 - 5000$ MeV ($m_b^{QCD} \sim$ 4.0–4.5 GeV)

$g \sim 700$ MeV ($m_g^{QCD} = 0$)

Exotic states:

$qq\bar{q}\bar{q}$ – 4-quarks states

$(q\bar{q})(q\bar{q})$ – molecule

$q\bar{q}$ + π's cloud

$q\bar{q}g$ – hibrid

gg – glueball

$\ldots$

$$\begin{pmatrix} q\bar{q} \\ qq\bar{q}\bar{q} \\ (q\bar{q})(q\bar{q}) \\ q\bar{q} + \pi \\ q\bar{q}g \\ gg \\ \ldots \end{pmatrix}$$

Systematics of the $q\bar{q}$-states on the (n, M^2) and (J, M^2) planes.

The analysis of the experimental data on the $p\bar{p}$ annihilation in flight with the production of mesons in the final state resulted in a discovery of a large number of mesons over the region 1900–2400 MeV:

[1] A.V. Anisovich, C.A. Baker, C.J. Batty *et al.*, Phys. Lett. B**449**, 114 (1999); B**452**, 173 (1999); B **452**, 180 (1999); B **452**, 187 (1999); B **472**, 168 (2000); B **476**, 15 (2000); B **477**, 19 (2000); B **491**, 40 (2000); B **491**, 47 (2000); B **496**, 145 (2000); B **507**, 23 (2001); B **508**, 6 (2001); B **513**, 281 (2001); B **517**, 261 (2001); B **517**, 273 (2001); Nucl. Phys. A **651**, 253 (1999); A **662**, 319 (2000); A **662**, 344 (2000).

This allows us to systematize quark-antiquark states on the (n, M^2) and (J, M^2) planes. The data point to almost linear meson trajectories on these planes, with a universal slope.

A.V. Anisovich, V.V. Anisovich, and A.V. Sarantsev, Phys. Rev. D **62**:051502 (2000),
A.V. Anisovich, V.V. Anisovich, V.A. Nikonov, and A.V. Sarantsev, *'Meson spectrum from analysis of the Crystal Barrel data'*, in: *'PNPI XXX, Scientific Highlights, Theoretical Physics Division'*, p. 58, Gatchina (2001),
V.V. Anisovich, UFN **174**,49 (2004) [Physics-Uspekhi **47**,45 (2004)].

In terms of $q\bar{q}$-states, the mesons form the nonets ${}^{2S+1}L_J$:

$$
\begin{aligned}
{}^1S_0 &\;\rightarrow\; \pi(10^{-+}),\; \eta(00^{-+})\;; \\
{}^3S_1 &\;\rightarrow\; \rho(11^{--}),\; \omega(01^{--})/\phi(01^{--})\;; \\
{}^1P_1 &\;\rightarrow\; b_1(11^{+-}),\; h_1(01^{+-})\;; \\
{}^3P_J &\;\rightarrow\; a_J(1J^{++}),\; f_J(0J^{++}),\; J=0,1,2\;; \\
{}^1D_2 &\;\rightarrow\; \pi_2(12^{-+}),\; \eta_2(02^{-+})\;; \\
{}^3D_J &\;\rightarrow\; \rho_J(1J^{--}),\; \omega_J(0J^{--})/\phi_J(0J^{--}),\; J=1,2,3\;; \\
{}^1F_3 &\;\rightarrow\; b_3(13^{+-}),\; h_3(03^{+-})\;; \\
{}^3F_J &\;\rightarrow\; a_J(1J^{++}),\; f_J(0J^{++}),\; J=2,3,4\,.
\end{aligned}
$$

Mesons ($I = 1$, $spin = 0$) on (n, M^2) plane $\quad M^2 = M_0^2 + \mu^2(n-1)$

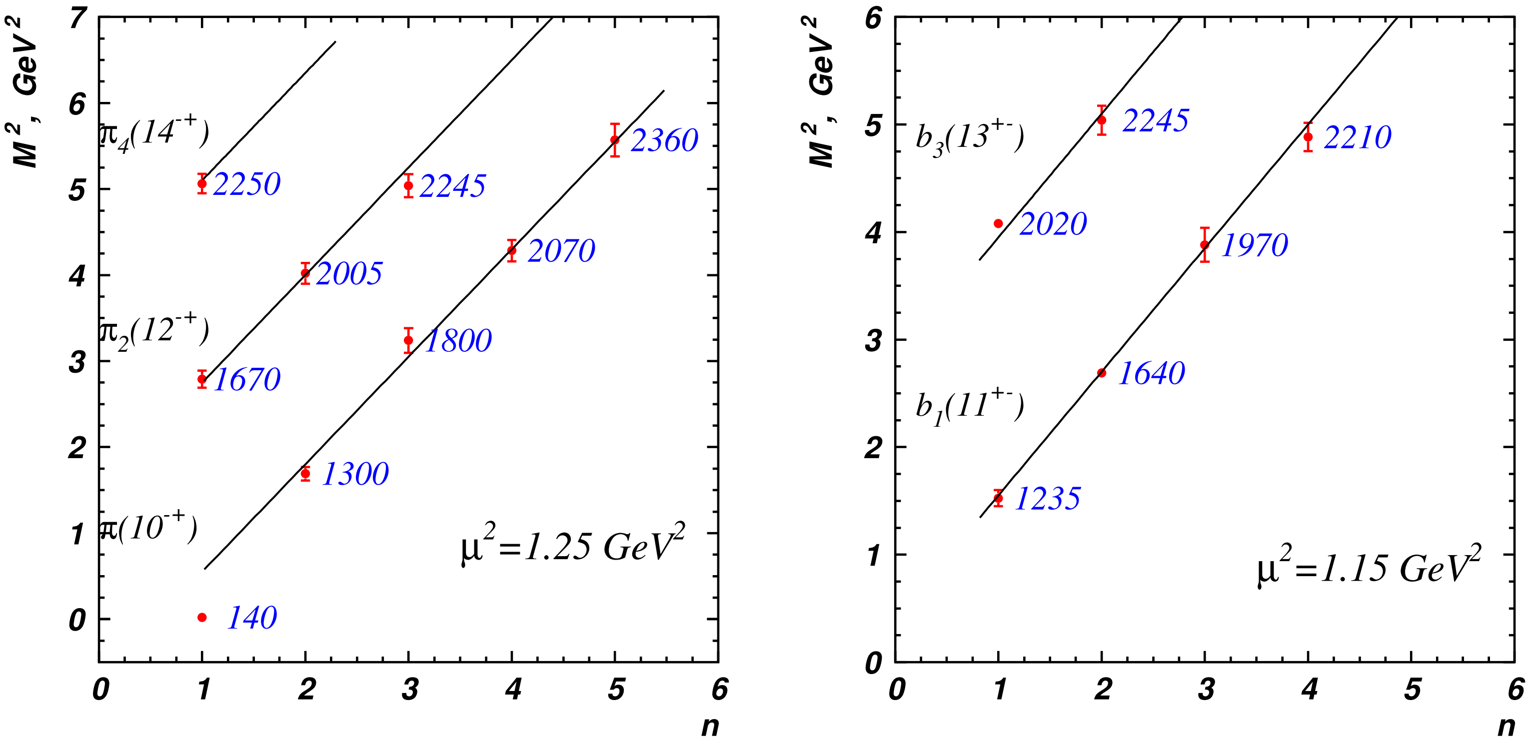

$$
\begin{array}{ll}
\pi\ (10^{-+})\ {}^1S_0\quad q\bar{q}\quad (L=0) & b_1(11^{+-})\ {}^1P_1\quad q\bar{q}\quad (L=1) \\
\pi_2(12^{-+})\ {}^1D_2\quad q\bar{q}\quad (L=2) & b_3(13^{+-})\ {}^1F_3\quad q\bar{q}\quad (L=3) \\
\pi_4(14^{-+})\ {}^1G_4\quad q\bar{q}\quad (L=4) & b_J(IJ^{PC})\ {}^{2s+1}L_J \\
\pi_J(IJ^{PC})\ {}^{2s+1}L_J &
\end{array}
\tag{1}
$$

Mesons ($I = 1$, $spin = 1$, L even) on (n, M^2) plane,

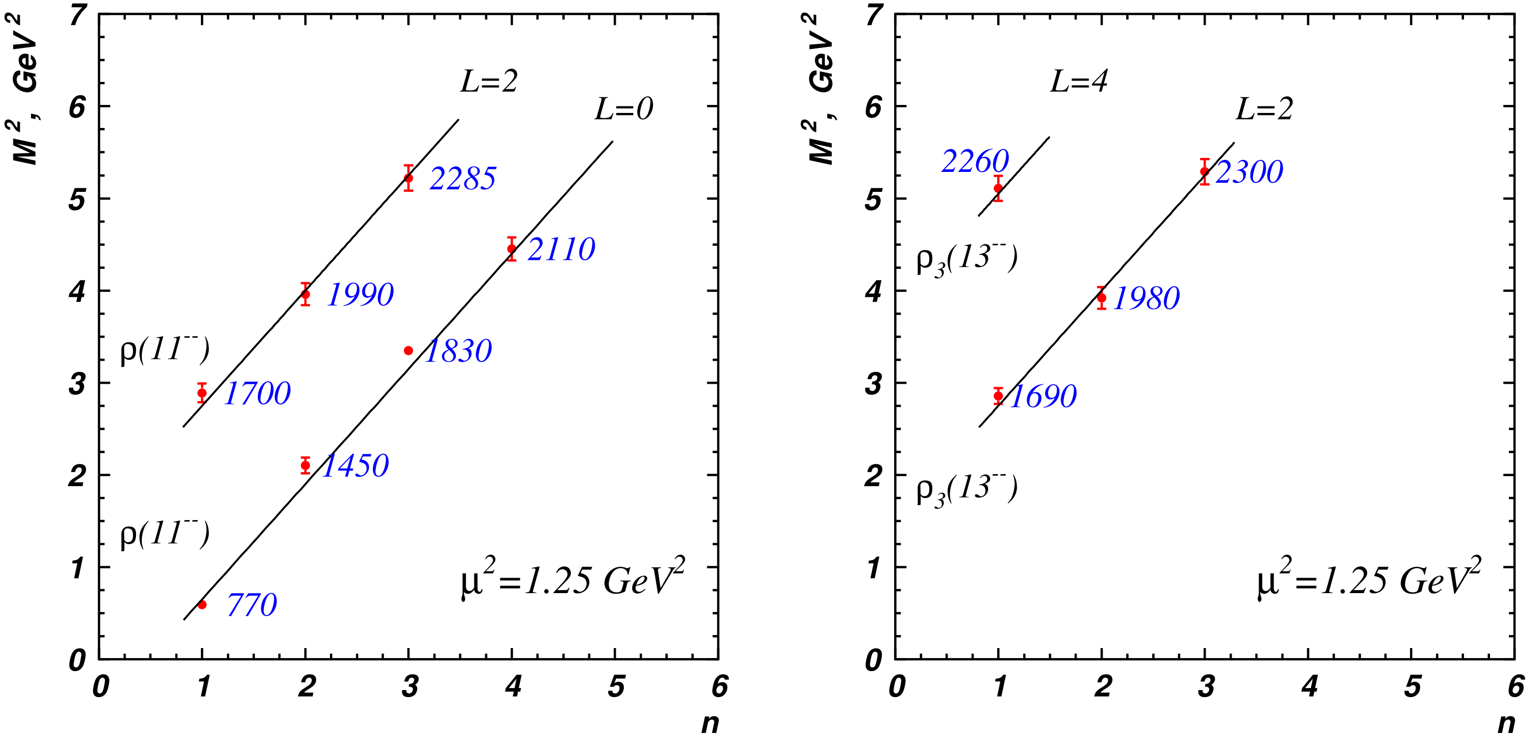

$$\rho(11^{--})\,{}^3S_1 \quad q\bar{q} \quad (L=0)$$

$$\rho(11^{--})\,{}^3D_1 \quad q\bar{q} \quad (L=2)$$

$$\rho_J(IJ^{PC})\,{}^{2s+1}L_J$$

$$\rho_3(13^{--})\,{}^3D_3 \quad q\bar{q} \quad (L=2)$$

$$\rho_3(13^{--})\,{}^3G_3 \quad q\bar{q} \quad (L=4)$$

Mesons ($I=1$, $spin=1$, L odd) on (n, M^2) plane

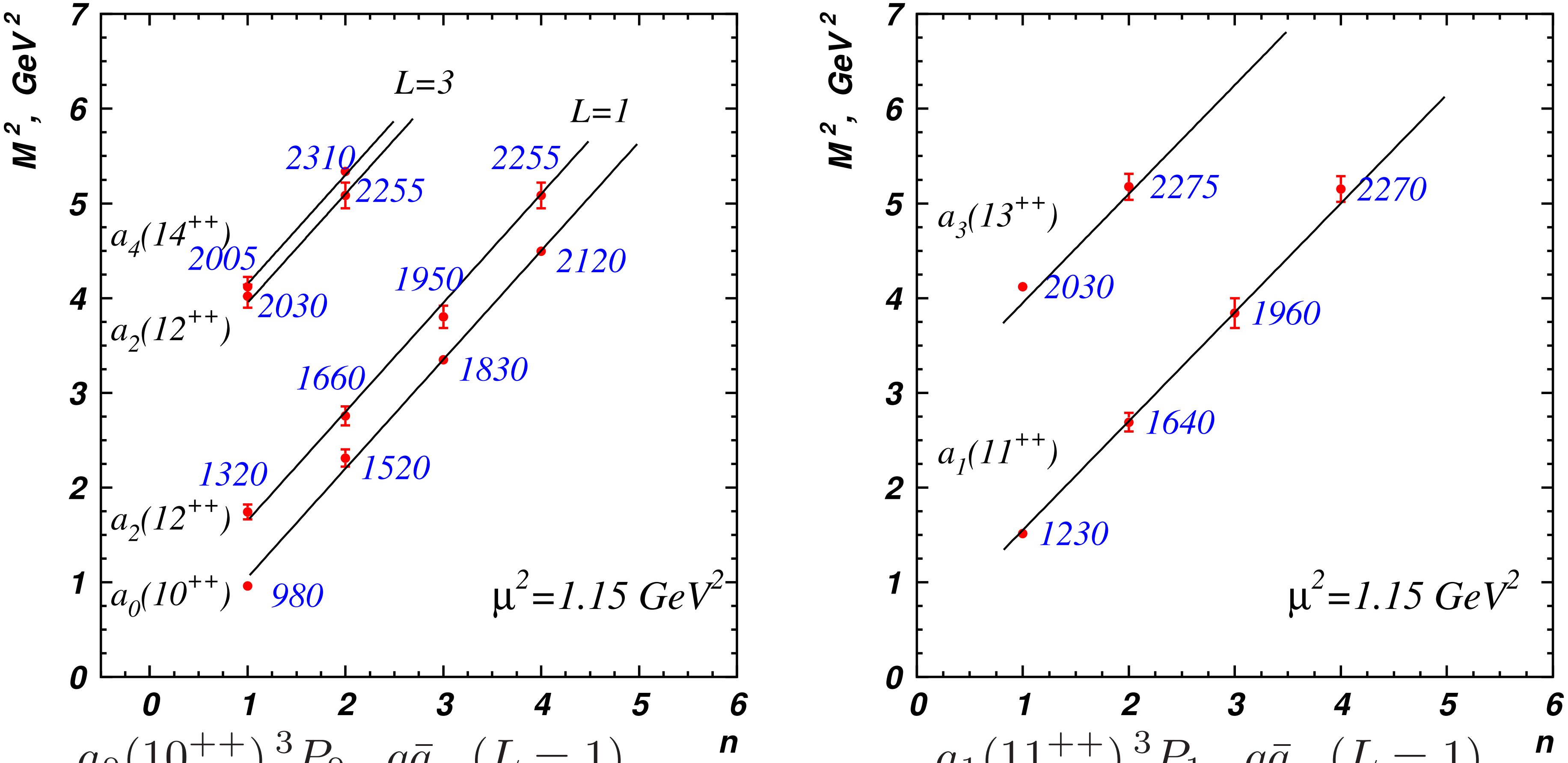

$a_0(10^{++})\ {}^3P_0 \quad q\bar{q} \quad (L=1)$

$a_2(12^{++})\ {}^3P_2 \quad q\bar{q} \quad (L=1)$

$a_2(12^{++})\ {}^3F_2 \quad q\bar{q} \quad (L=3)$

$a_4(14^{++})\ {}^3F_4 \quad q\bar{q} \quad (L=3)$

$a_1(11^{++})\ {}^3P_1 \quad q\bar{q} \quad (L=1)$

$a_3(13^{++})\ {}^3F_3 \quad q\bar{q} \quad (L=3)$

$a_J(IJ^{PC})\ {}^{2s+1}L_J$

Mesons ($I = 0$, $spin = 1$) on (n, M^2) plane. Scalar glueball $f_0(1200-1600)$, tensor glueball $f_2(2000)$.

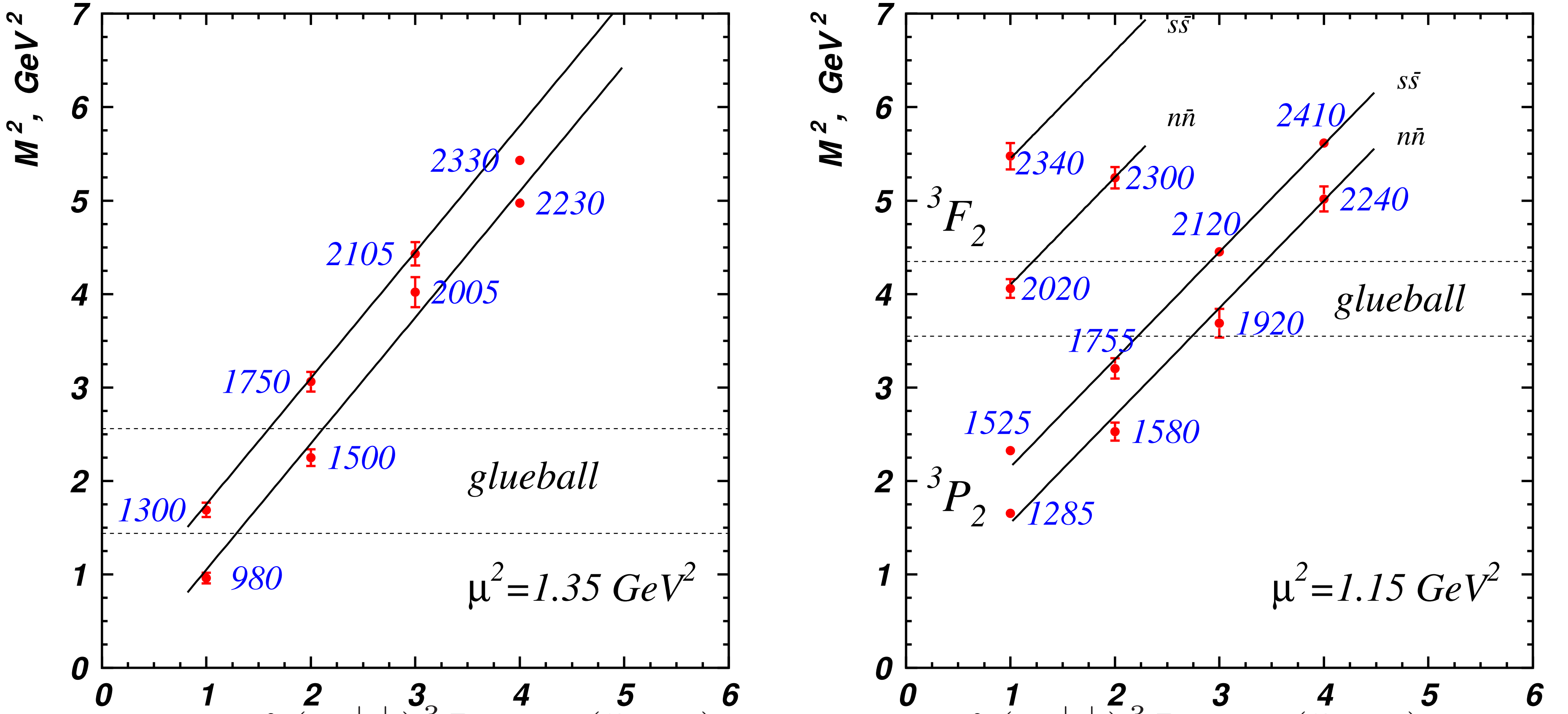

$f_0(00^{++})\,^3P_0 \quad q\bar{q} \quad (L=1)$ **n**

$f_J(0J^{++})\,^3L_J$

$f_2(02^{++})\,^3P_2 \quad q\bar{q} \quad (L=1)$ **n**

$f_2(02^{++})\,^3F_2 \quad q\bar{q} \quad (L=3)$

$$(1) \quad \cos\varphi\, n\bar{n} + \sin\varphi\, s\bar{s}\,, (2) \quad -\sin\varphi\, n\bar{n} + \cos\varphi\, s\bar{s}$$

Mesons ($I = 0$, $spin = 0$) on (n, M^2) plane,

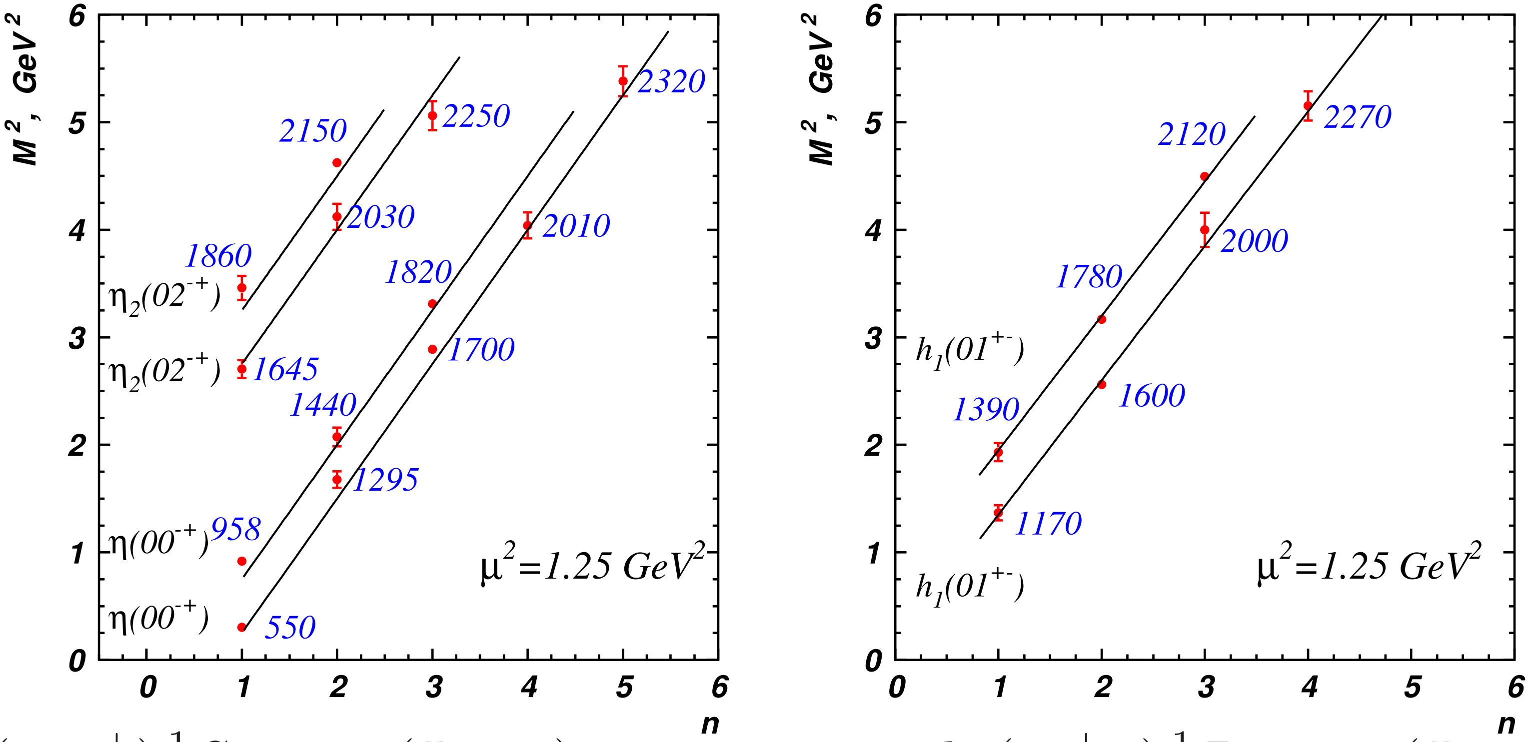

$\eta\ (00^{-+})\ {}^1S_0\quad q\bar{q}\quad (L=0)$

$h_1(01^{+-})\ {}^1P_1\quad q\bar{q}\quad (L=1)$

$\eta_2(02^{-+})\ {}^1D_2\quad q\bar{q}\quad (L=2)$

$$n\bar{n} + s\bar{s}$$

Mesons ($I = 0$, $spin = 1$) on (n, M^2) plane,

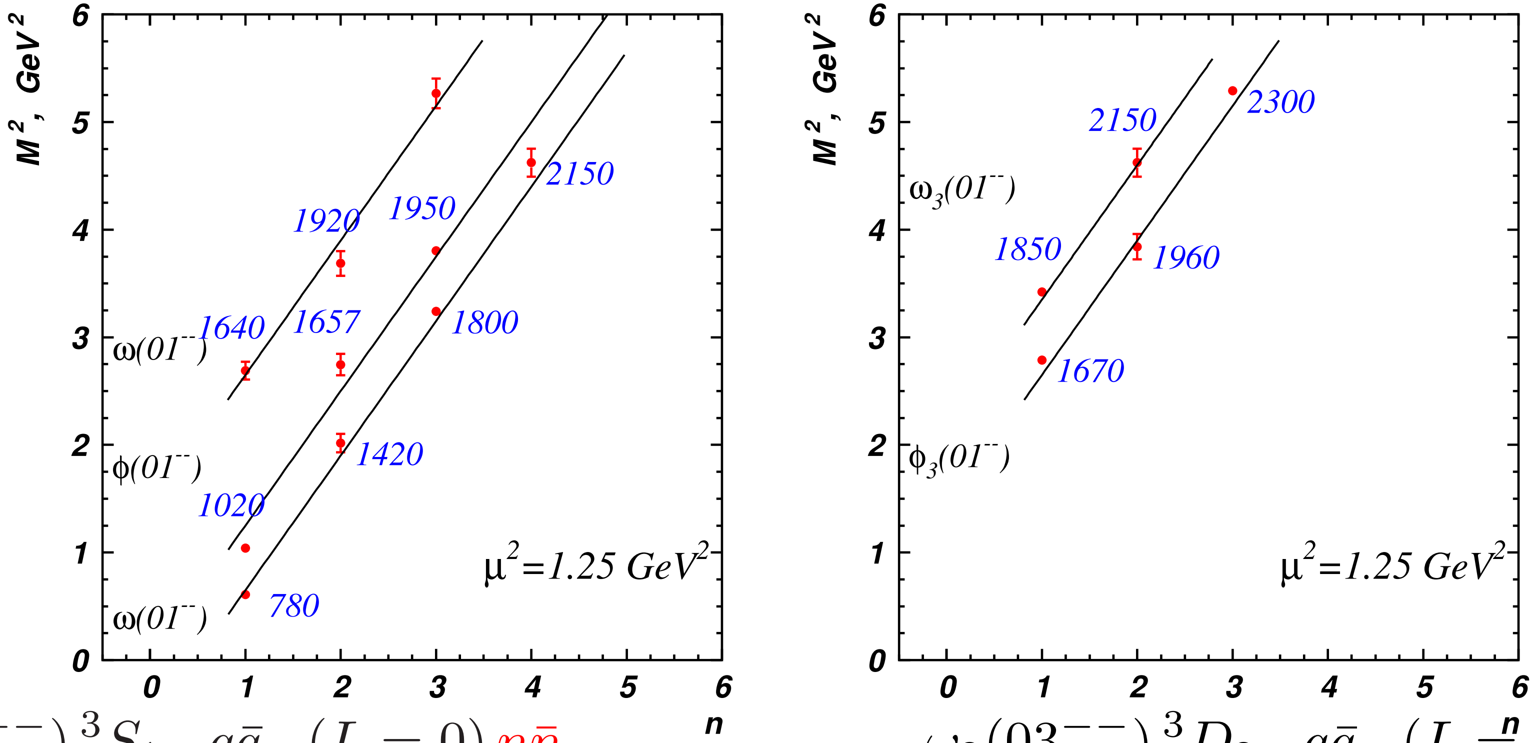

$\omega(01^{--})\,^3S_1 \quad q\bar{q} \quad (L=0)\; n\bar{n}$

$\phi(01^{--})\,^3S_1 \quad q\bar{q} \quad (L=0)\; s\bar{s}$

$\omega(01^{--})\,^3D_1 \quad q\bar{q} \quad (L=2)\; n\bar{n}$

$\omega_3(03^{--})\,^3D_3 \quad q\bar{q} \quad (L=2)\; n\bar{n}$

$\phi_3(03^{--})\,^3D_3 \quad q\bar{q} \quad (L=2)\; s\bar{s}$

$$\omega, \phi_J(IJ^{--})\,^{2s+1}L_J$$

Trajectories on the (J, M^2) plane:

pion trajectory and the daugther ones, a_1-meson and the daugther ones.

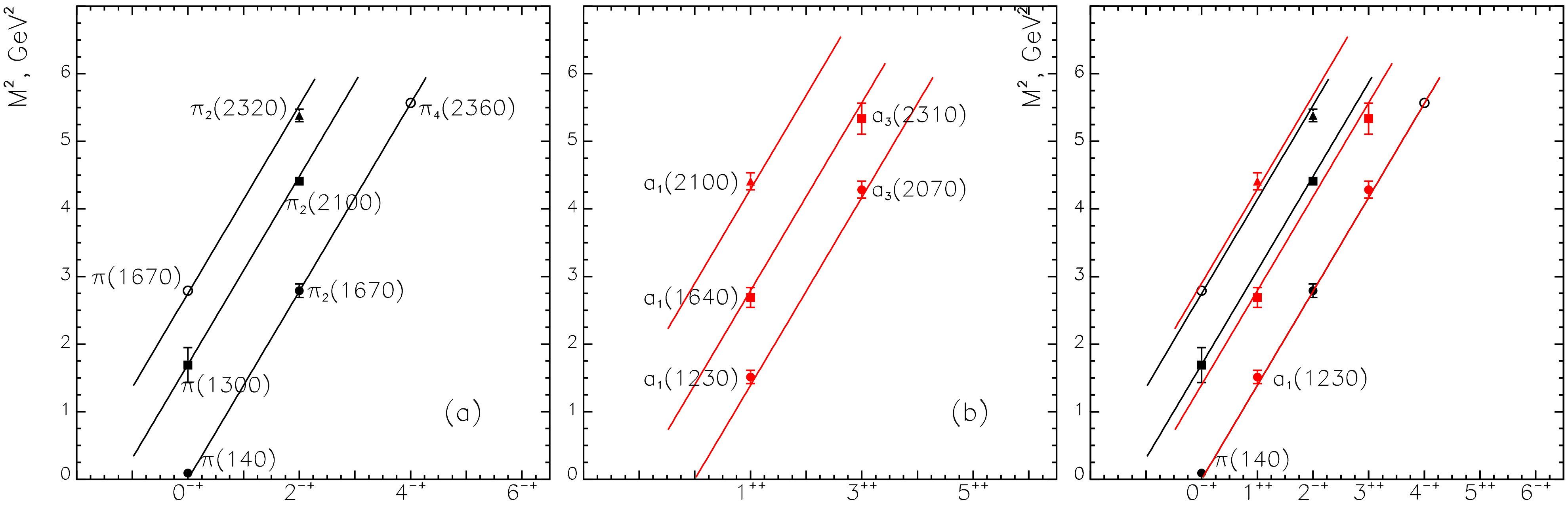

Degeneracy of the

π and a_1 trajectories,

combined presentation.

Trajectories on the (J, M^2) plane:

ρ-meson and daugther trajectories,

a_2-meson and daugther trajectories.

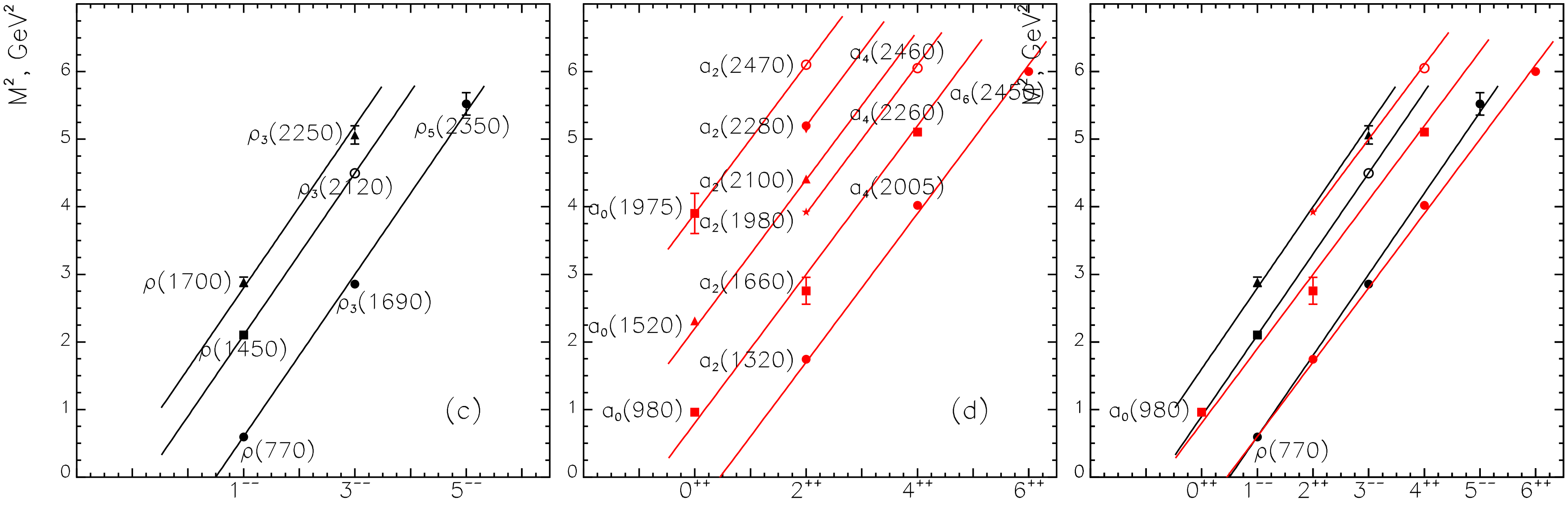

Combined presentation:

ρ and a_2 trajectories are degenerate. $a_0(980)$ is on the daughter trajectory.

If $a_0(980)$ is not a $q\bar{q}$ state, there should be another a_0 in the mass region $\sim$ 1000 MeV.

Trajectories on the (J, M^2) plane:

f_2-meson and daugther trajectories,

ω-meson and daugther trajectories.

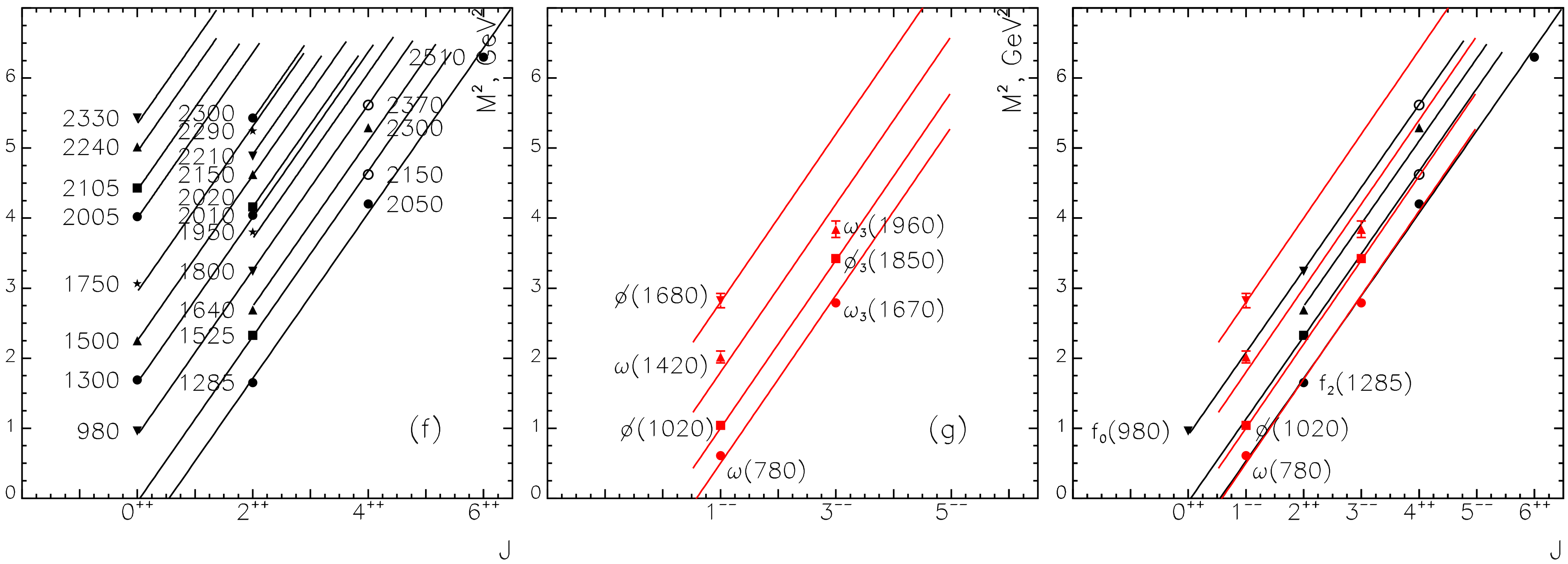

Combined presentation:

$f_0(980)$ belongs to the $q\bar{q}$ trajectory.

Baryon trajectories on the (n, M^2) plane:

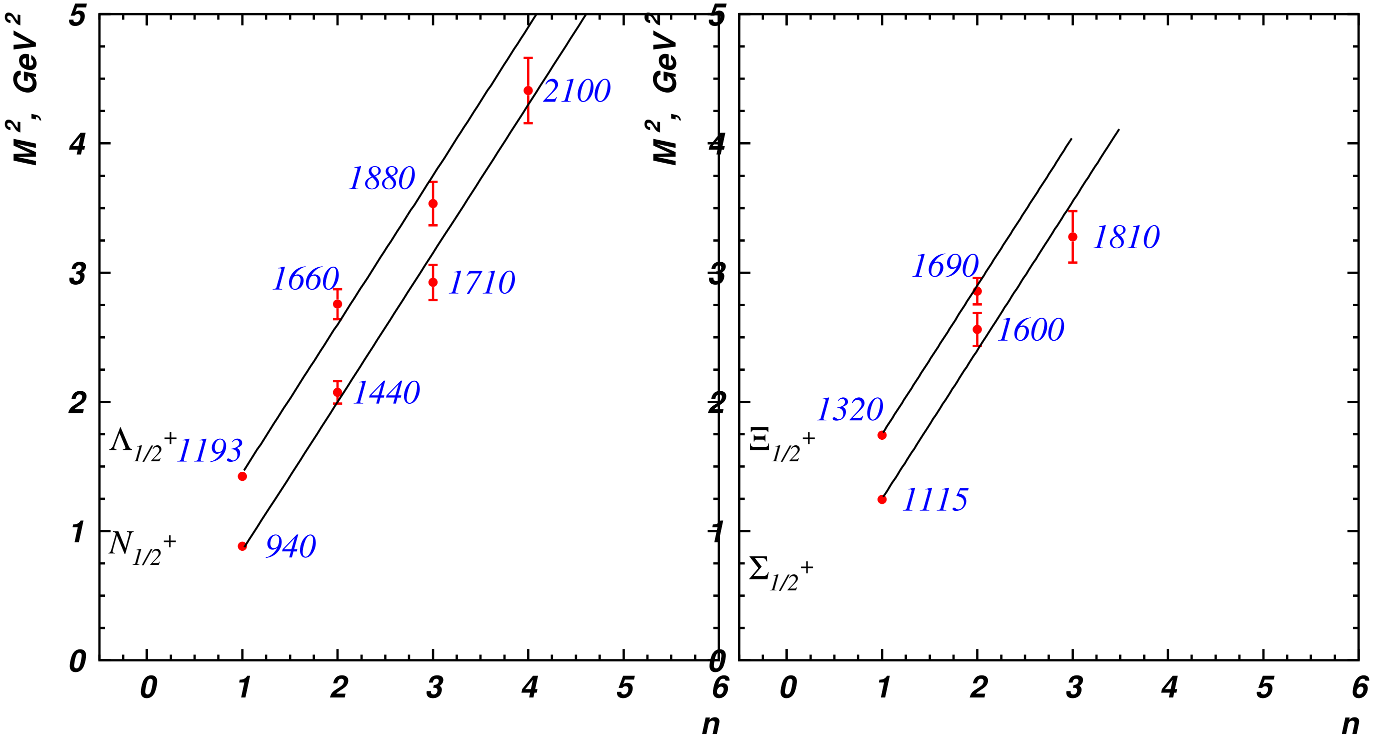

Baryon trajectories on the (n, M^2) plane:

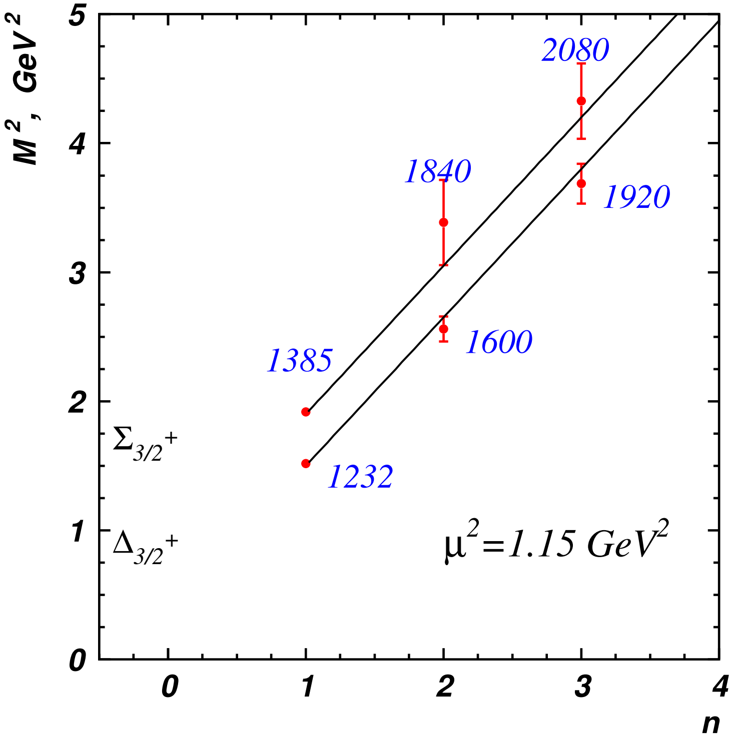

1. Spectral integral equation (N/D-equation with separable vertex).

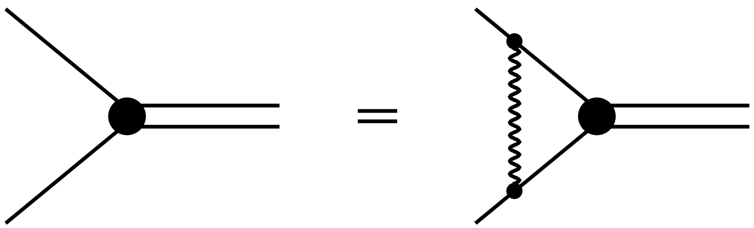

$$(s-M^2)\psi(s)=\int\limits_{4m^2}^{\infty}\frac{ds'}{\pi}\int d\Phi(k')V\left(s,s',(kk')\right)\psi(s')\,.$$

2. Radiative transitions: $(q\bar q)_{in}\to\gamma+(q\bar q)_{out}$, $(q\bar q)\to\gamma\gamma$, $e^+e^-\to(q\bar q)$

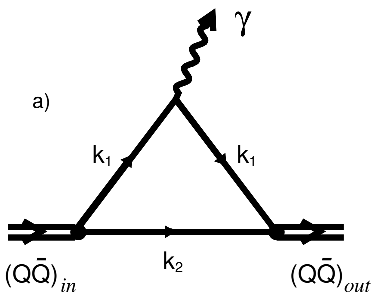

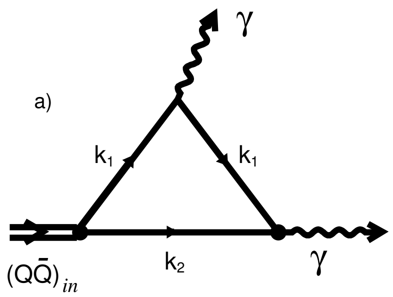

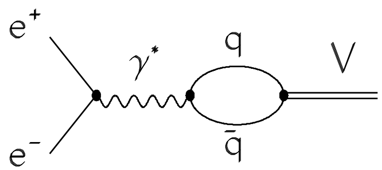

Spectral representation of equation for vertex $(Q\bar{Q})_{meson} \to Q\bar{Q}$

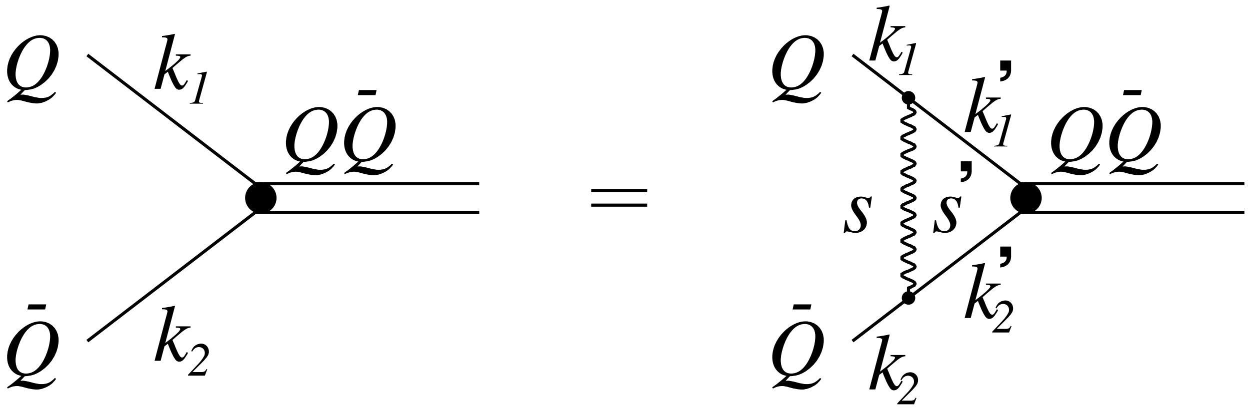

(i) energy does not conserved, $s \neq s'$

(ii) quarks on-mass-shell, $k_1'^2 = k_2'^2 = m^2$

Instantaneous interaction: $\widehat{V}\left(s, s', (k_\perp k'_\perp)\right) \longrightarrow \widehat{V}(t_\perp)$

Interaction with retardation: $\widehat{V}\left(s, s', (kk')\right) \longrightarrow \widehat{V}(t)$

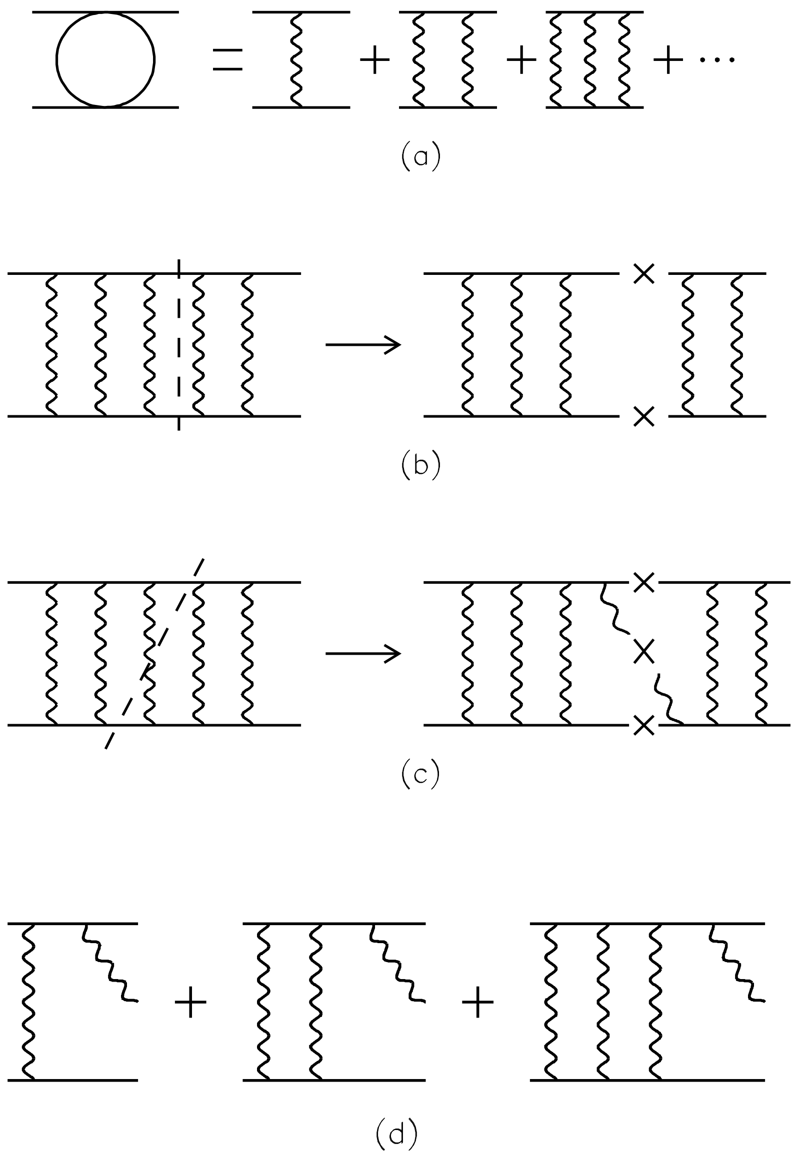

a) Presentation of the scattering amplitude as a set of the ladder diagrams with the t-channel meson exchange interaction; b,c) cuttings of the ladder diagrams;

d) meson production processes which are determined by ladder diagrams.

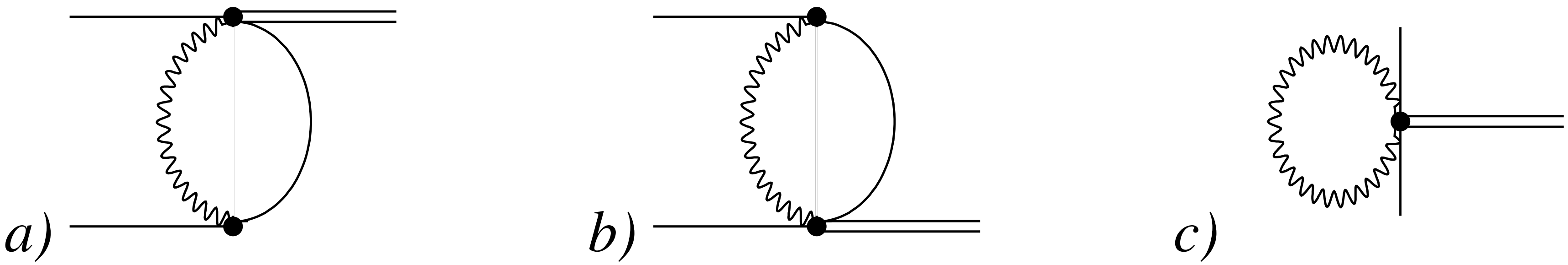
a)
b)
c)

Interaction block.Coordinate representation of interaction

$$I_N^{(coor)}(r,\mu) = r^N\ e^{-\mu r}$$

$$V(r) = a + b\,r + c\,e^{-\mu_c\ r} + d\frac{e^{-\mu_d\ r}}{r}.$$

Momentum representation of interaction:

$$I_{-1} = \frac{4\pi}{\mu^2 - t}, \qquad I_1 = 8\pi\left(\frac{4\mu^2}{(\mu^2+t)^3} - \frac{1}{(\mu^2-t)^2}\right),$$

$$I_0 = \frac{8\pi\mu}{(\mu^2-t)^2}, \qquad I_2 = 96\pi\mu\left(\frac{2\mu^2}{(\mu^2-t)^4} - \frac{1}{(\mu^2-t)^3}\right)$$

μ_a (constant term a) and μ_b (linear term b) are chosen to be small enough: $1 - 10$ MeV.

$$\psi_{(n)}^{(S,L,J)}(k^2) = e^{-\beta k^2}\sum_{i=1}^{9} c_i(S,L,J;n)k^{i-1},$$

where $k^2 \equiv \mathbf{k}^2$ ($s = 4m^2 + 4\mathbf{k}^2$). $\beta = 1.2$ GeV^{-2}.

Interaction	Wave	a	b	c	μ_c	d	μ_d
	$L=0$	-2.860	0.150	5.057	0.410	0.221	0.410
	$L=1$	-0.398	0.150	5.362	0.410	-2.270	0.210
$(\mathrm{I}\otimes\mathrm{I})$	$L=2$	8.407	0.150	6.866	0.110	-1.250	0.210
	$L=3$	-0.281	0.150	5.243	0.110	-32.507	0.410
	$L=4$	-1.912	0.150	3.8574	0.010	-3.3175	0.110
	$L=0$	0.180	-0.150	0.060	0.610	0.656	0.010
	$L=1$	0.971	-0.150	-1.888	0.610	0.664	0.010
$(\gamma_\mu\otimes\gamma_\mu)$	$L=2$	1.804	-0.150	-2.135	0.610	0.405	0.010
	$L=3$	1.239	-0.150	-12.823	0.710	0.588	0.010
	$L=4$	1.548	-0.150	-2.5458	0.210	0.536	0.010

The fit requires the confinement terms $V_{conf}(r)$ for both scalar, $(I\otimes I)$, and vector, $(\gamma_\mu\otimes\gamma_\mu)$, exchanges, and the slopes of the potentials turn out to be approximately the same: $b_S\simeq -b_V$. In the final fit, we fix the slopes to be equal thus obtaining $b_S=|b_V|=0.15$ GeV^2. In this way, one can see that the spin structure of the confinement potential has rather nice form as follows:

$$[I\otimes I-\gamma_\mu\otimes\gamma_\mu]_{t-\mathrm{channel}}\ . \tag{2}$$

$q\bar{q}\ L = 0, 2$

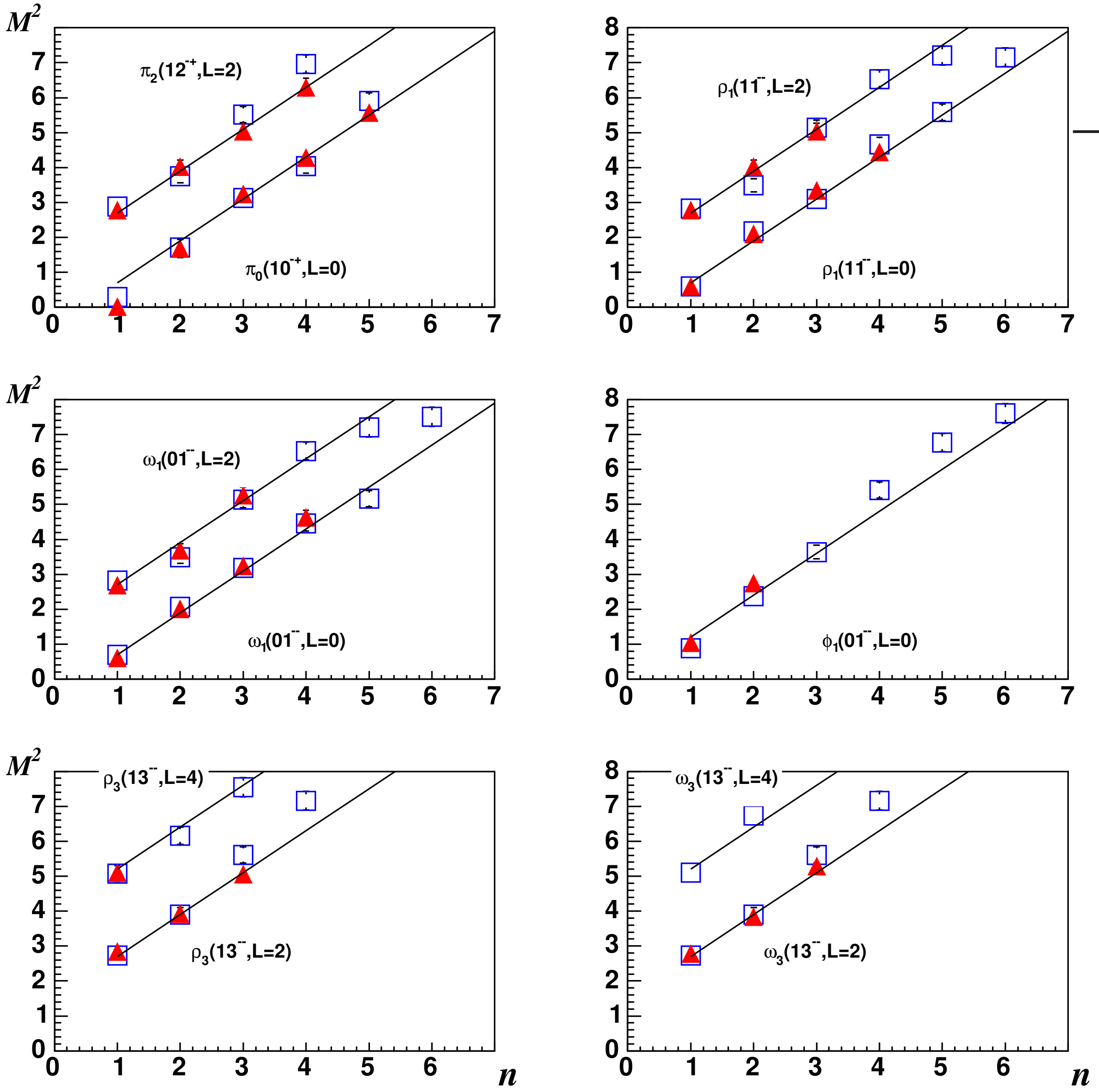

Process	Data (keV)	Fit (keV)
$\pi(1S) \to \gamma\gamma$	0.007	0.005
$\pi(2S) \to \gamma\gamma$	—	3.742
$\pi(3S) \to \gamma\gamma$	—	8.466
$\rho(770) \to e^+e^-$	7.02±0.11	6.583
$\rho(1450) \to e^+e^-$	—	1.416
$\rho(1830) \to e^+e^-$	—	0.964
$\rho(2110) \to e^+e^-$	—	0.974
$\omega(780) \to e^+e^-$	0.60±0.02	0.776
$\omega(1420) \to e^+e^-$	—	0.388
$\omega(1800) \to e^+e^-$	—	0.326
$\omega(2150) \to e^+e^-$	—	0.255
$\phi(1020) \to e^+e^-$	1.27±0.04	1.353
$\phi(1657) \to e^+e^-$	—	0.985

$q\bar{q}$ $L = 1$

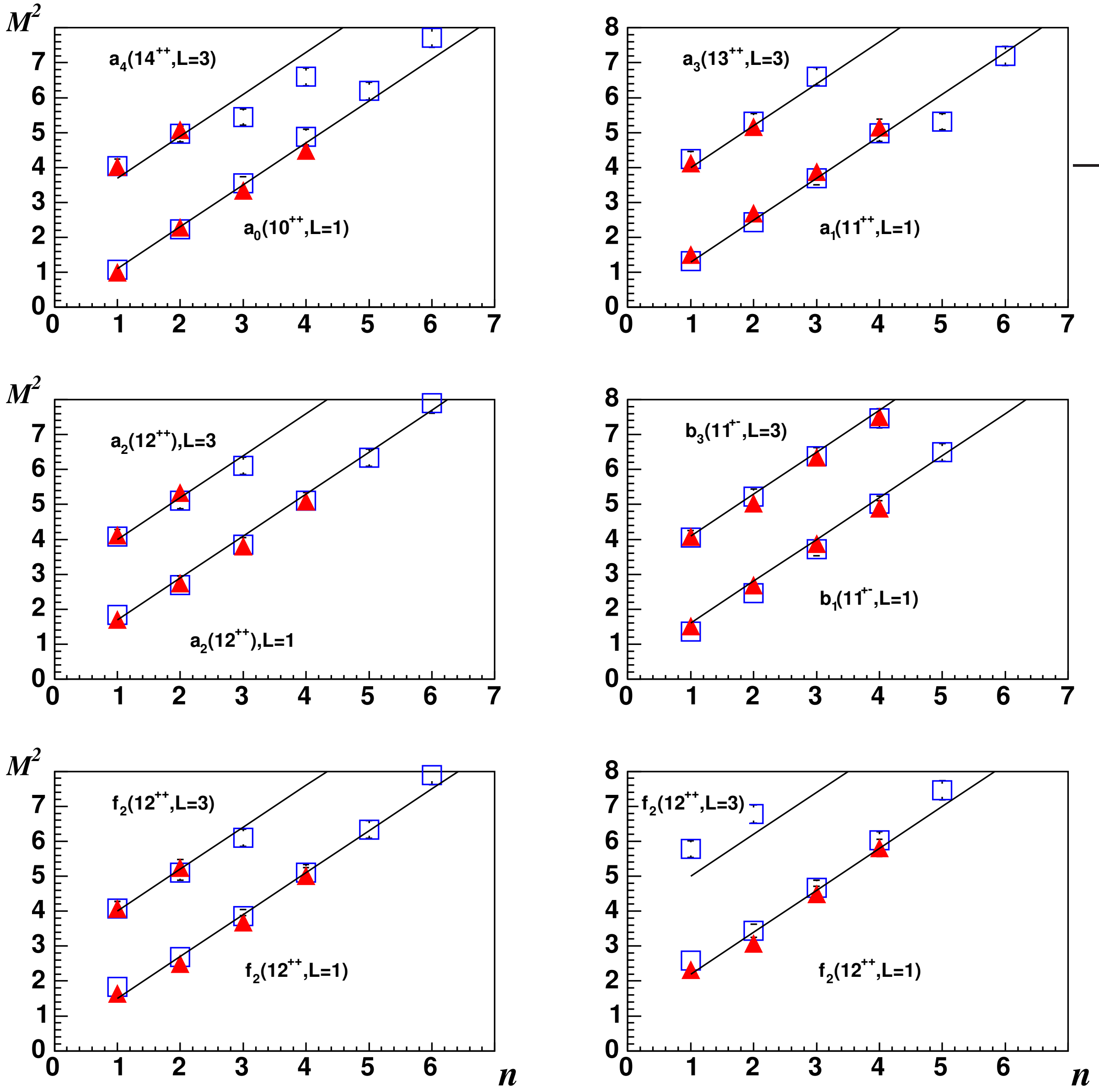

Process	Data (keV)	Fit (keV)
$a_0(1P) \to \gamma\gamma$	0.300±0.100	0.340
$a_0(2P) \to \gamma\gamma$	—	0.224
$a_0(3P) \to \gamma\gamma$	—	0.186
$a_2(1P) \to \gamma\gamma$	1.00±0.06	1.045
$a_2(2P) \to \gamma\gamma$	—	0.821
$a_2(3P) \to \gamma\gamma$	—	0.699
$f_2(1P)(n\bar{n}) \to \gamma\gamma$	2.590±0.3	2.946
$f_2(2P)(n\bar{n}) \to \gamma\gamma$	—	2.396
$f_2(3P)(n\bar{n}) \to \gamma\gamma$	—	1.971
$f_2(1P)(s\bar{s}) \to \gamma\gamma$	0.100±0.02	0.135
$f_2(2P)(s\bar{s}) \to \gamma\gamma$	—	0.118
$f_2(3P)(s\bar{s}) \to \gamma\gamma$	—	0.097

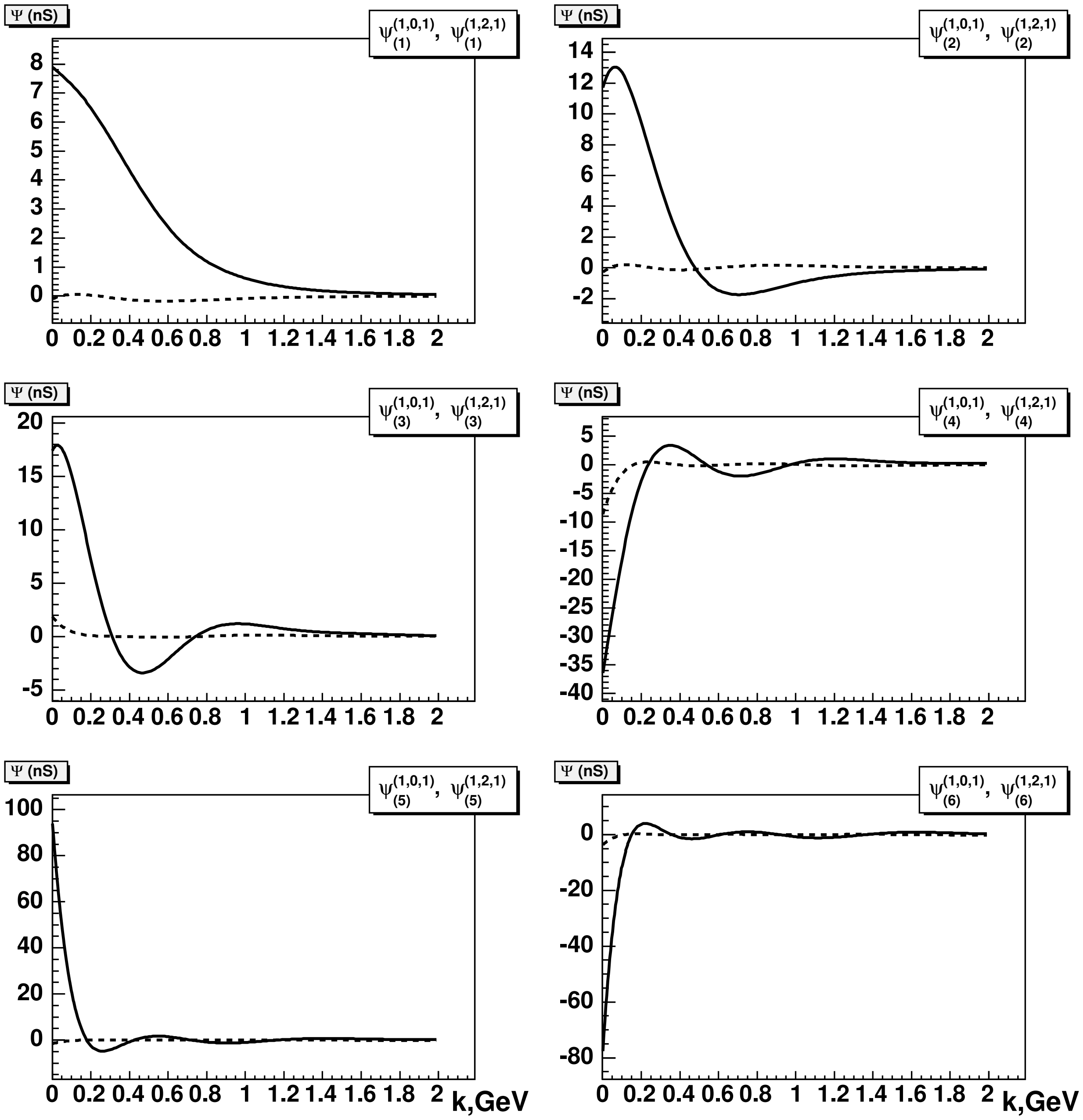
Ψ (nS)
$\psi^{(1,0,1)}_{(1)}$, $\psi^{(1,2,1)}_{(1)}$
$\psi^{(1,0,1)}_{(2)}$, $\psi^{(1,2,1)}_{(2)}$
$\psi^{(1,0,1)}_{(3)}$, $\psi^{(1,2,1)}_{(3)}$
$\psi^{(1,0,1)}_{(4)}$, $\psi^{(1,2,1)}_{(4)}$
$\psi^{(1,0,1)}_{(5)}$, $\psi^{(1,2,1)}_{(5)}$
$\psi^{(1,0,1)}_{(6)}$, $\psi^{(1,2,1)}_{(6)}$
k,GeV

Heavy quarkonium: $c\bar{c}$-sector

Solving spectral integral equation, the known levels were included into fitting procedure:

$$J^{PC} = 0^{-+}, 1^{--}, 0^{++}, 1^{++}, 2^{++}, 2^{-+}, n \le 6,$$

together with radiative transitions

$$J/\psi \to \gamma\eta_{c0}(1S) \qquad \chi_{cJ}(1P) \to \gamma J/\psi \qquad \psi(2S) \to \gamma\eta_{c0}(1S)$$
$$\psi(2S) \to \gamma\chi_{cJ}(1P) \qquad J = 0, 1, 2.$$

The $c\bar{c}$ component of the photon wave function was defined using the transitions

$$e^+e^- \to J/\psi(3097), \psi(3686), \psi(3770), \psi(4040), \psi(4160), \psi(4415)$$

and calculate partial widths of the two-photon decays of the $1S, 1P$ states:

$$\eta_{c0}(2979), \chi_{c0}(3415), \chi_{c2}(3556) \to \gamma\gamma,$$

and $2S, 2P$ states:

$$\eta_{c0}(3594) \to \gamma\gamma, \chi_{c0}(3849), \chi_{c2}(3950) \to \gamma\gamma.$$

The predictions are also given for the two-photon decays $\eta_{c0}, \chi_{c0}, \chi_{c2} \to \gamma\gamma$ of other states with $n \le 6$. m_c is taken to be 1.25 GeV.

Quark–Antiquark States and their Radiative Decays

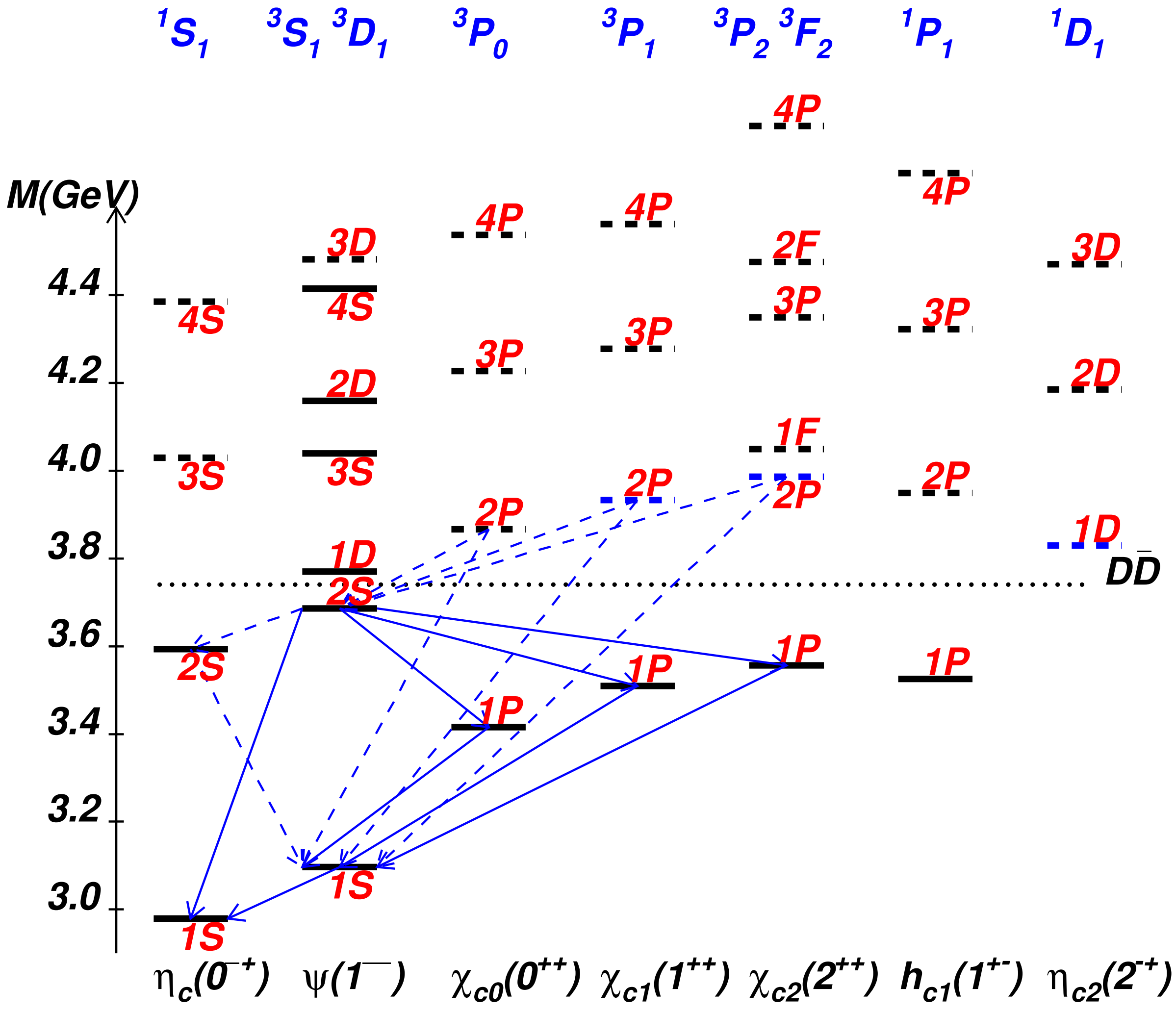

The recently observed states $X(3872)$ and $Y(3941)$ [Choi (Belle Collab.),Acosta (CDF II Collab.), Abrazov (D0 Collab.), Aubert (Barbar Collab.)] are lively discussed at present time.

[N.A. Törnqvist, arXiv:hep-ph/0402237; F.E. Close and P.R. Page, Phys. Lett. B **578**, 119 (2004); M.B. Voloshin, Phys. Lett.B **579**, 316 (2004); C.Z. Yuan, X.M. Mo and P. Wang, Phys. Lett. B **579**,74 (2004); C.-Y. Wong, Phys. Rev. C **69**, 055202 (2004); T. Barnes and S. Godfrey, Phys. Rev. D **69**, 054008 (2004); E.S. Swanson, Phys. Lett. B **588**, 189 (2004). T. Skwarnicki, arXiv:hep-ph/0311243. P. Bicudo, arXiv:hep-ph/0401106. E.J. Eichten, K. Lane and C. Quigg, Phys. Rev. D **69**, 094019 (2004)].

Our calculations favour

$X(3872)$ is either the excited 1^{++}-state $\chi_{c1}(2P)$, or basic 2^{-+}-state $\eta_{c2}(1D)$,

$Y(3941)$ can be radial excited 2^{++} state, $\chi_{c2}(2P)$.

Parameters for the $c\bar{c}$-state potential:

Interaction	Solution	a	b	c	μ_c	d	μ_d
$(\mathrm{I}\otimes\mathrm{I})$	$I(c\bar{c})$	-1.980	0.172	1.141	0.201	0.000	0.401
	$II(c\bar{c})$	-1.980	0.172	1.597	0.201	0.000	0.401
	$U(c\bar{c})$	-0.300	0.210	-1.691	0.201	0.521	0.401
	$R(c\bar{c})$	-1.551	0.157	0.952	0.201	0.000	0.401
$(\gamma_\mu\otimes\gamma_\mu)$	$I(c\bar{c})$	-1.682	0.000	1.225	0.201	0.506	0.001
	$II(c\bar{c})$	-1.682	0.000	1.587	0.201	0.445	0.001
	$U(c\bar{c})$	1.000	-0.130	-2.855	0.201	1.105	0.001
	$R(c\bar{c})$	-1.312	0.000	0.977	0.201	0.492	0.001

$$V(r) = a + b\,r + c\,e^{-\mu_c\,r} + d\frac{e^{-\mu_d\,r}}{r}$$

e^+e^- - annihilation

Process	Data	$I(c\bar{c})$	$II(c\bar{c})$	$U(c\bar{c})$	$R(c\bar{c})$
$J/\psi(1S) \to e^+e^-$	5.40 ± 0.22	5.392	5.360	5.403	6.088
$\psi(2S) \to e^+e^-$	2.14 ± 0.21	2.146	2.137	2.142	2.843
$\psi(1D) \to e^+e^-$	0.24 ± 0.05	0.239	0.730	0.240	0.301
$\psi(3S) \to e^+e^-$	0.75 ± 0.15	0.754	0.472	0.749	1.210
$\psi(2D) \to e^+e^-$	0.47 ± 0.10	0.472	0.236	0.469	0.113
$\psi(4S) \to e^+e^-$	0.77 ± 0.23	0.771	0.763	0.770	0.915

Radiative transitions: comparison to data

Process	Data	$I(c\bar{c})$	$II(c\bar{c})$	$U(c\bar{c})$	$R(c\bar{c})$
$J/\psi(1S) \to \gamma\eta_{c0}(1S)$	1.1$\pm$0.3	2.877	4.853	1.274	4.216
$\chi_{c0}(1P) \to \gamma J/\psi$	165$\pm$50	180.845	164.884	253.894	180.578
$\chi_{c1}(1P) \to \gamma J/\psi$	295$\pm$90	291.536	297.362	386.110	289.569
$\chi_{c2}(1P) \to \gamma J/\psi$	390$\pm$120	226.700	239.835	278.851	225.265
$\eta_{c0}(2S) \to \gamma J/\psi$	—	23.297	23.326	40.263	25.852
$\psi(2S) \to \gamma\eta_{c0}(1S)$	0.8$\pm$0.2	1.661	2.529	1.724	2.309
$\psi(2S) \to \gamma\chi_{c0}(1P)$	26$\pm$4	22.854	32.408	28.973	22.169
$\psi(2S) \to \gamma\chi_{c1}(1P)$	25$\pm$4	45.291	51.853	66.095	44.343
$\psi(2S) \to \gamma\chi_{c2}(1P)$	20$\pm$4	26.096	20.929	83.077	26.620
$\psi(2S) \to \gamma\eta_{c0}(2S)$	—	0.541	0.770	1.003	0.447

Radiative transitions: predictions

Process	Data	$I(c\bar{c})$	$II(c\bar{c})$	$U(c\bar{c})$	$R(c\bar{c})$
$\chi_{c0}(2P) \to \gamma J/\psi$	—	9.181	5.841	0.468	12.612
$\chi_{c1}(2P) \to \gamma J/\psi$	—	48.130	50.831	28.797	59.013
$\chi_{c2}(2P) \to \gamma J/\psi$	—	56.911	72.080	31.331	67.713
$\chi_{c0}(2P) \to \gamma\psi(2S)$	—	81.851	73.158	92.450	73.925
$\chi_{c1}(2P) \to \gamma\psi(2S)$	—	212.937	221.604	290.379	192.502
$\chi_{c2}(2P) \to \gamma\psi(2S)$	—	154.796	176.599	197.162	144.714

Transitions $c\bar{c} \to 2\gamma$: comparison to data

Process	Data	$I(c\bar{c})$	$II(c\bar{c})$	$U(c\bar{c})$	$R(c\bar{c})$
$\eta_{c0}(1S) \to \gamma\gamma$	7.0$\pm$0.9	6.971	6.808	7.002	7.088
$\chi_{c0}(1P) \to \gamma\gamma$	2.6$\pm$0.5	2.426	2.620	2.578	2.212
$\chi_{c2}(1P) \to \gamma\gamma$	1.02$\pm$0.40$\pm$0.17(L3)	0.558	0.528	0.068	5.706
	1.76$\pm$0.47$\pm$0.40(OPAL)				
	1.08$\pm$0.30$\pm$0.26(CLEO)				
	0.33$\pm$0.08$\pm$0.06(E760)				

Transitions $c\bar{c} \to 2\gamma$: predictions

Process	Data	$I(c\bar{c})$	$II(c\bar{c})$	$U(c\bar{c})$	$R(c\bar{c})$
$\eta_{c0}(2S) \to \gamma\gamma$	—	12.234	11.947	12.289	12.439
$\chi_{c0}(2P) \to \gamma\gamma$	—	2.142	2.313	2.276	1.953
$\chi_{c2}(2P) \to \gamma\gamma$	—	0.500	0.473	0.061	5.111

Comparison of data for the transitions $(c\bar{c})_{in} \longrightarrow \gamma + (c\bar{c})_{out}$ with our results and calculations of other groups (the width is given in keV).

Decay	Data	$I(c\bar{c})$	LS(F)[1]	LS(C)[1]	RM(S)[2]	RM(V)[2]	NR[3]
$J/\psi(1S) \to \eta_{c0}(1S)\gamma$	1.1±0.3	3.4	1.7–1.3	1.7–1.4	3.35	2.66	1.21
$\psi(2S) \to \chi_{c0}(1P)\gamma$	26±4	23	31–47	26–31	31	32	19.4
$\psi(2S) \to \chi_{c1}(1P)\gamma$	25±4	45	58–49	63–50	36	48	34.8
$\psi(2S) \to \chi_{c2}(1P)\gamma$	20±4	26	48–47	51–49	60	35	29.3
$\psi(2S) \to \eta_{c0}(1S)\gamma$	0.8±0.2	2.0	11–10	10–13	6	1.3	4.47
$\chi_{c0}(1P) \to J/\psi(1S)\gamma$	165±50	181	130–96	143–110	140	119	147
$\chi_{c1}(1P) \to J/\psi(1S)\gamma$	295±90	292	390–399	426–434	250	230	287
$\chi_{c2}(1P) \to J/\psi(1S)\gamma$	390±120	227	218–195	240–218	270	347	393

[1] Relativistic Bethe–Salpeter equation, instantaneous forces, Feynman and Coulomb gauges. [2] Relativistic Bethe–Salpeter equation, instantaneous forces, different forms of vector forces. [3] Nonrelativistic Bethe–Salpeter equation.

Decay widths $\psi \to e^+e^-$, our results and those of other groups v.s. data (in keV).

Decay	Data	$I(c\bar{c})$	LS(F)[1]	LS(C)[1]	RM(S)[2]	RM(V)[2]	NR[3]
$J/\psi(1S) \to e^+e^-$	5.40 ± 0.22	5.39	5.26	5.26	8.05	9.21	12.2
$\psi(2S) \to e^+e^-$	2.14 ± 0.21	2.15	2.8–2.5	2.9–2.7	4.30	5.87	4.63
$\psi(1D) \to e^+e^-$	0.24 ± 0.05	0.24	2.0–1.6	2.1–1.8	3.05	4.81	3.20
$\psi(3S) \to e^+e^-$	0.75 ± 0.15	0.75	1.4–1.0	1.6–1.3	2.16	3.95	2.41
$\psi(2D) \to e^+e^-$	0.47 ± 0.10	0.47	—	—	—	—	—
$\psi(4S) \to e^+e^-$	0.77 ± 0.23	0.77	—	—	—	—	—

[1] J. Linde and H. Snellman, Nucl. Phys. A **619**, 346 (1997). [2] J. Resag and C.R. Münz, Nucl. Phys. A **590**, 735 (1995). [3] M.Beyer, U. Bohn, M.G. Huber, B.C. Metsch, and J. Resag, Z.Phys C **55**, 307 (1992).

Decay widhs $(c\bar{c})_{in} \to \gamma + (c\bar{c})_{out}$ in the region below 4 GeV (in keV)

Decay	Data	$I(c\bar{c})$	LS[1]	[4]	[5]	[6]	[7]	[8]	[9]
$\eta_c(1S) \to \gamma\gamma$	7.0±0.9	6.9	6.2–6.3 (F,C)	5.5	3.5	10.9	7.8	5.5	4.8
$\eta_c(1S) \to \gamma\gamma$	—	12.2	–	1.8	1.38	–	3.5	2.1	3.7
$\chi_{c0}(1P) \to \gamma\gamma$	2.6±0.5	2.4	1.5–1.8 (F,C)	2.9	1.39	6.4	2.5	5.32	–
$\chi_{c0}(1P) \to \gamma\gamma$	—	2.1	—	1.9	1.11	–	–	–	–
$\chi_{c2}(1P) \to \gamma\gamma$	1.02±0.40±0.17[L3] 1.76±0.47±0.40[OPAL] 1.08±0.30±0.26[CLEO] 0.33±0.08±0.06[E760]	0.61	0.3–0.4 (F,C)	0.50	0.44	0.57	0.28	0.44	–
$\chi_{c2}(1P) \to \gamma\gamma$	—	0.5	—	0.52	0.48	–	–	–	–

[1] Linde, [4]D. Ebert, R.N. Faustov, and V.O. Galkin, Phys. Rev D **67**, 014027 (2003), [5] S.N. Münz, Nucl. Rhys. A **609**, 364 (1996), [6] S.N. Gupta, S.F. Radford, and W.W. Repko, Phys. Rev. D **54**, 2075 (1996), [7] G.A. Schuler, F.A Berends, and R. van Gulik, Nucl. Rhys. B **523**, 423 (1998), [8] H.-W. Huang, *et. al.* Phys. Rev. D **54**, 2123 (1996); D **56**, 368 (1997), [9] E.S. Ackleh, T. Barnes, *et al.,* Phys. Rev. D **45**, 232 (1992).

Heavy quarkonium: $b\bar{b}$-sector

We reconstruct the interaction in $b\bar{b}$-sector on the basis of

1. data for the levels of bottomonium states with following quantum numbers:

$$J^{PC} = 0^{-+}, 1^{--}, 0^{++}, 1^{++}, 1^{+-}, 2^{++}$$

at the radial quantum numbers $n \le 6$

2. their wave functions are obtained by solving spectral integral equation together with fitting to radiative transition data

$$\Upsilon(3S) \to \gamma\chi_{bJ}(2P) \qquad \Upsilon(2S) \to \gamma\chi_{bJ}(1P); \qquad J = 0, 1, 2.$$

Soft component of the $b\bar{b}$ photon wave function was determined from the e^+e^- annihilation data:

$$e^+e^- \to \Upsilon(9460), \Upsilon(10023), \Upsilon(10355), \Upsilon(10580), \Upsilon(10865), \Upsilon(11019).$$

Partial widths of the two-photon decays were predicted for

$$\eta_{b0} \to \gamma\gamma,\ \chi_{b0} \to \gamma\gamma,\ \chi_{b2} \to \gamma\gamma$$

.

$m_b = 4.5$ GeV.

Quark–Antiquark States and their Radiative Decays

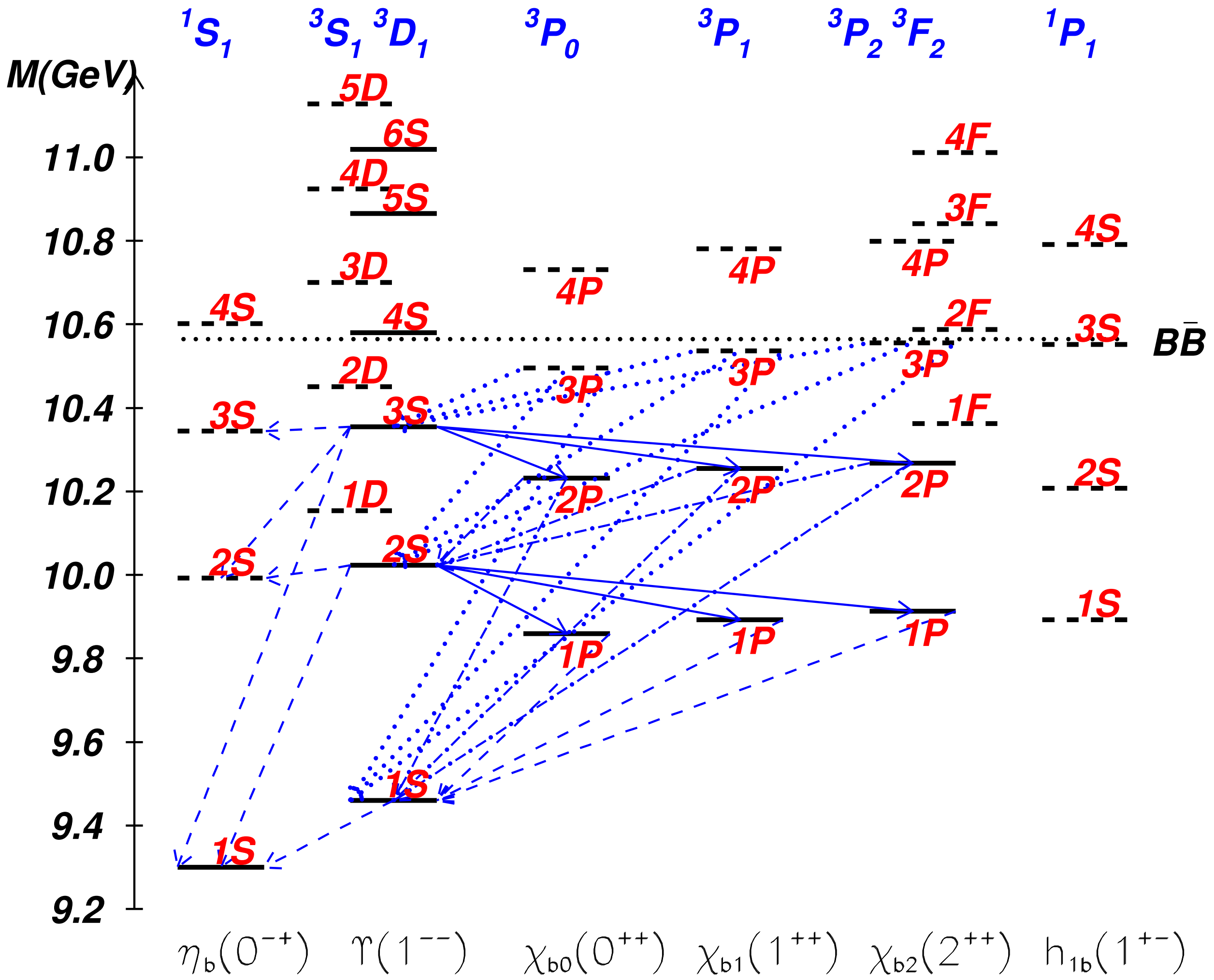

II $b\bar{b}$ sector

Parameters for the $b\bar{b}$-state potential:

Interaction	Wave	a	b	c	μ_c	d	μ_d
	$I(b\bar{b})$	-0.845	0.174	0.098	0.201	0.219	0.401
$(\mathrm{I} \otimes \mathrm{I})$	$U(b\bar{b})$	-0.210	0.271	-0.643	0.201	0.280	0.401
	$R(b\bar{b})$	-0.680	0.130	1.322	0.201	-0.228	0.401
	$I(b\bar{b})$	-1.549	0.000	0.376	0.201	0.671	0.001
$(\gamma_\mu \otimes \gamma_\mu)$	$U(b\bar{b})$	0.700	-0.094	-2.550	0.201	1.026	0.001
	$R(b\bar{b})$	-1.620	-0.005	1.821	0.201	0.311	0.001

$$V(r) = a + b\,r + c\,e^{-\mu_c\,r} + d\frac{e^{-\mu_d\,r}}{r}$$

Radiative decays: comparison to data

Process	Data	$I(b\bar{b})$	$U(b\bar{b})$	$R(b\bar{b})$	E1[1]	E1[2]
$\Upsilon(1S) \to \gamma\eta_{b0}(1S)$	—	0.010	0.028	0.008	—	—
$\Upsilon(2S) \to \gamma\eta_{b0}(1S)$	—	0.017	0.037	0.001	—	—
$\Upsilon(2S) \to \gamma\eta_{b0}(2S)$	—	0.001	0.001	0.001	—	—
$\Upsilon(2S) \to \gamma\chi_{b0}(1P)$	1.7±0.2	1.289	0.910	0.961	1.62	1.41
$\Upsilon(2S) \to \gamma\chi_{b1}(1P)$	3.0±0.5	2.637	1.354	2.126	2.55	2.27
$\Upsilon(2S) \to \gamma\chi_{b2}(1P)$	3.1±0.5	2.203	1.099	1.936	2.51	2.24
$\Upsilon(3S) \to \gamma\eta_{b0}(1S)$	—	0.016	0.033	0.001	—	—
$\Upsilon(3S) \to \gamma\eta_{b0}(2S)$	—	0.004	0.003	0.001	—	—
$\Upsilon(3S) \to \gamma\eta_{b0}(3S)$	—	0.001	0.001	0.001	—	—
$\Upsilon(3S) \to \gamma\chi_{b0}(2P)$	1.4±0.2	1.667	1.446	1.125	1.77	—
$\Upsilon(3S) \to \gamma\chi_{b1}(2P)$	3.0±0.5	3.129	3.206	3.127	2.88	—
$\Upsilon(3S) \to \gamma\chi_{b2}(2P)$	3.0±0.5	3.563	2.746	3.168	3.14	—

[2]J.H. Kühn, preprint MPI-PAE/PTh 25/88 (1988).

[1]J. Resag and C.R. Münz, Nucl. Phys. A **590**, 735 (1995).

Process	Data	$I(b\bar{b})$	$U(b\bar{b})$	$R(b\bar{b})$
$\chi_{b0}(1P) \to \gamma\Upsilon(1S)$	—	24.225	33.202	34.468
$\chi_{b1}(1P) \to \gamma\Upsilon(1S)$	—	30.105	38.806	42.624
$\chi_{b2}(1P) \to \gamma\Upsilon(1S)$	—	26.222	31.509	38.105
$\chi_{b0}(2P) \to \gamma\Upsilon(1S)$	$\Gamma_{tot}(\chi_{b0}(2P)) \cdot (0.9 \pm 0.6) \cdot 10^{-2}$	2.679	6.142	7.080
$\chi_{b0}(2P) \to \gamma\Upsilon(2S)$	$\Gamma_{tot}(\chi_{b0}(2P)) \cdot (4.6 \pm 2.1) \cdot 10^{-2}$	9.021	11.477	11.063
$\chi_{b1}(2P) \to \gamma\Upsilon(1S)$	$\Gamma_{tot}(\chi_{b1}(2P)) \cdot (8.5 \pm 1.3) \cdot 10^{-2}$	1.034	12.587	11.695
$\chi_{b1}(2P) \to \gamma\Upsilon(2S)$	$\Gamma_{tot}(\chi_{b1}(2P)) \cdot (21.0 \pm 4.0) \cdot 10^{-2}$	3.644	17.689	16.018
$\chi_{b2}(2P) \to \gamma\Upsilon(1S)$	$\Gamma_{tot}(\chi_{b2}(2P)) \cdot (7.1 \pm 1.0) \cdot 10^{-2}$	7.438	12.880	12.370
$\chi_{b2}(2P) \to \gamma\Upsilon(2S)$	$\Gamma_{tot}(\chi_{b2}(2P)) \cdot (16.2 \pm 2.4) \cdot 10^{-2}$	13.903	15.290	14.410

Process	Data	$I(b\bar{b})$	$U(b\bar{b})$	$R(b\bar{b})$
$\chi_{b0}(3P) \to \gamma\Upsilon(1S)$	—	0.104	2.454	2.844
$\chi_{b1}(3P) \to \gamma\Upsilon(1S)$	—	5.501	6.467	5.430
$\chi_{b2}(3P) \to \gamma\Upsilon(1S)$	—	0.006	7.546	6.011
$\chi_{b0}(3P) \to \gamma\Upsilon(2S)$	—	0.419	0.997	2.046
$\chi_{b1}(3P) \to \gamma\Upsilon(2S)$	—	11.773	3.461	4.095
$\chi_{b2}(3P) \to \gamma\Upsilon(2S)$	—	0.011	4.514	4.574
$\chi_{b0}(3P) \to \gamma\Upsilon(3S)$	—	0.390	9.247	7.195
$\chi_{b1}(3P) \to \gamma\Upsilon(3S)$	—	0.000	15.881	11.331
$\chi_{b2}(3P) \to \gamma\Upsilon(3S)$	—	0.203	13.936	9.873

$$\begin{aligned}
\Gamma_{tot}(\chi_{b0}(1P)) &\quad < \quad 400\,\mathrm{keV}, \\
\Gamma_{tot}(\chi_{b1}(1P)) &\quad \simeq \quad 70 - 130\,\mathrm{keV}, \\
\Gamma_{tot}(\chi_{b2}(1P)) &\quad \simeq \quad 80 - 120\,\mathrm{keV}, \\
\Gamma_{tot}(\chi_{b0}(2P)) &\quad \simeq \quad 100 - 300\,\mathrm{keV}, \\
\Gamma_{tot}(\chi_{b1}(2P)) &\quad \simeq \quad 10 - 20\,\mathrm{keV}, \\
\Gamma_{tot}(\chi_{b2}(2P)) &\quad \simeq \quad 70 - 120\,\mathrm{keV}.
\end{aligned} \tag{3}$$

Process	Data	$I(b\bar{b})$	$U(b\bar{b})$	$R(b\bar{b})$
$\eta_{b0}(2S) \to \gamma\Upsilon(1S)$	—	0.184	0.309	0.117
$\eta_{b0}(3S) \to \gamma\Upsilon(1S)$	—	0.234	0.361	0.109
$\eta_{b0}(3S) \to \gamma\Upsilon(2S)$	—	0.057	0.050	0.016

(4)

Conclusion

1. Masses and wave functions are defined.

2. The wave functions being known, radiative decays are calculated in agreement with experiment.

3. For the confinement potential (br), the scalar and vector forces are found to be equal to each other: $b_S = |b_V| = 0.15$ GeV^2 $(b_S \simeq -b_V)$.

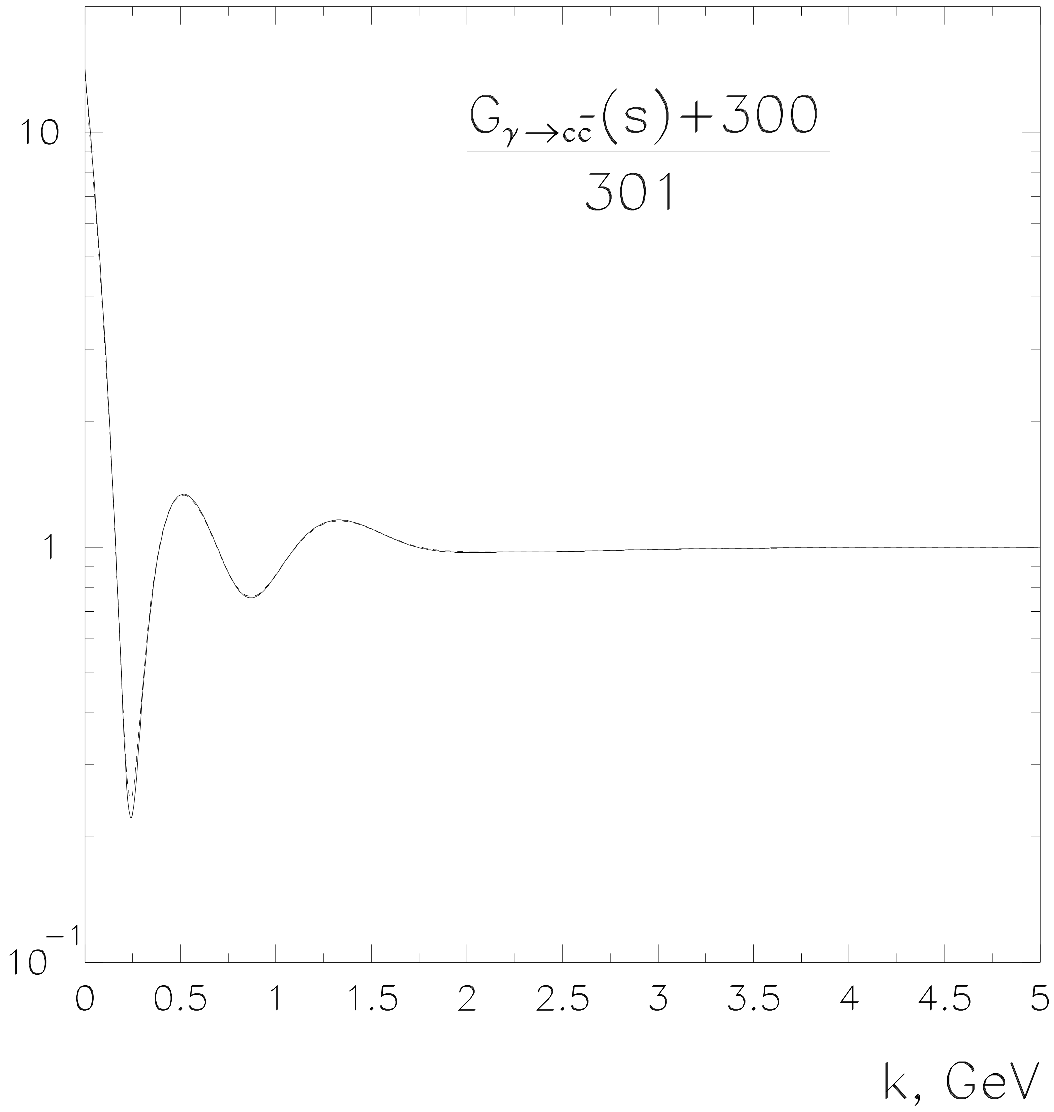
$\frac{G_{\gamma\to c\bar{c}}(s)+300}{301}$
10
1
10^{-1}
0
0.5
1
1.5
2
2.5
3
3.5
4
4.5
5
k, GeV

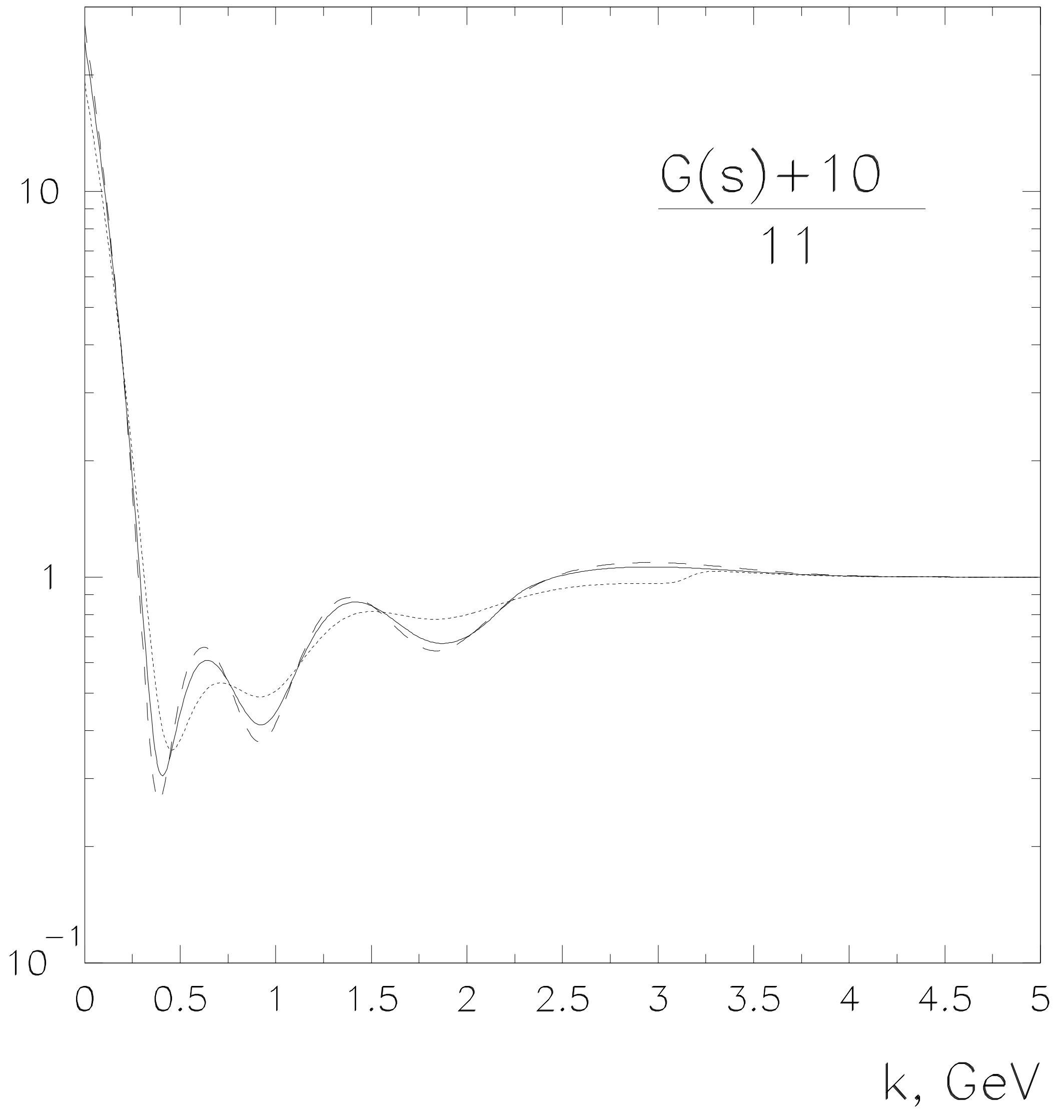

$\frac{G(s)+10}{11}$
10
1
10^{-1}
0
0.5
1
1.5
2
2.5
3
3.5
4
4.5
5
k, GeV

Basic equation and its solution:

$$(s-M^2)\psi(s)=\int\limits_{4m^2}^{\infty}\frac{ds'}{\pi}\int d\Phi(k')V\left(s,s',(kk')\right)\psi(s')\ .$$

With $\mathbf{k}'^2$ and $\mathbf{k}^2$ instead of s' and s, $\psi(s)\to\psi(\mathbf{k}^2)$,:

$$(4\mathbf{k}^2+4m^2-M^2)\psi(\mathbf{k}^2)=\int\frac{d^3\mathbf{k}'_1}{(2\pi)^3k'_0}V\left(s,s',-(\mathbf{k}\mathbf{k}')\right)\psi(\mathbf{k}'^2)\ .$$

! $L=0$. The set is formed by the levels with different radial excitations $n=1,2,3,...$, and relevant wave functions are $\psi_1(\mathbf{k}^2),\ \psi_2(\mathbf{k}^2),\ \psi_3(\mathbf{k}^2),...$. The wave functions are normalized and orthogonal to each other:

$$\int\frac{d^3\mathbf{k}}{(2\pi)^3k_0}\psi_n(\mathbf{k}^2)\psi_{n'}(\mathbf{k}^2)=\delta_{nn'}\ .$$

Spectral integral equation for the S-wave mesons:

$$4(\mathbf{k}^2+m^2)\psi_n(\mathbf{k}^2)-\int\limits_0^\infty \frac{d\mathbf{k}'^2}{\pi} V_0(\mathbf{k}^2,\mathbf{k}'^2)\phi(\mathbf{k}'^2)\psi_n(\mathbf{k}'^2)=M^2\psi_n(k^2)\ ,$$

where

$$\phi(\mathbf{k}'^2)=\frac{1}{4\pi}\frac{|\mathbf{k}'|}{k'_0}\ .$$

The $\psi_n(\mathbf{k}^2)$ presents a full set of wave functions which are orthogonal and normalized:

$$\int\limits_0^\infty \frac{d\mathbf{k}^2}{\pi}\psi_a(\mathbf{k}^2)\phi(k)\psi_b(\mathbf{k}^2)=\delta_{ab}\ .$$

The function $V_0(\mathbf{k}^2,\mathbf{k}'^2)$ is the projection of potential $V(s,s',(kk'))$ on the S-wave:

$$V_0(k,k')=\int\frac{d\Omega_{\mathbf{k}}}{4\pi}\int\frac{d\Omega_{\mathbf{k}'}}{4\pi}V\left(s,s',-(\mathbf{k}\mathbf{k}')\right)\ .$$

Let us expand $V_0(\mathbf{k}^2,\mathbf{k}'^2)$ with respect to full set of wave functions:

$$V_0(\mathbf{k}^2,\mathbf{k}'^2)=\sum_{a,b}\psi_a(\mathbf{k}^2)v^{(0)}_{ab}\psi_b(\mathbf{k}'^2)\ ,$$

where numerical coefficients $v^{(0)}_{ab}$ are defined by the inverse transformation as follows:

$$v^{(0)}_{ab}=\int\limits_0^\infty\frac{d\mathbf{k}^2}{\pi}\frac{d\mathbf{k}'^2}{\pi}\psi_a(\mathbf{k}^2)\phi(\mathbf{k}^2)V_0(\mathbf{k}^2,\mathbf{k}'^2)\phi(\mathbf{k}'^2)\psi_b(\mathbf{k}'^2)\ .$$

Matrix form of spectral integral equation:

$$4(\mathbf{k}^2+m^2)\psi_n(\mathbf{k}^2)-\sum_a\psi_a(\mathbf{k}^2)v^{(0)}_{an}=M^2\psi_n(k^2)\ .$$

Such a transformation should be carried out upon the kinetic-energy term, it is also expanded in a series with respect to a full set of wave functions:

$$4(\mathbf{k}^2+m^2)\psi_n(\mathbf{k}^2)=\sum_a K_{na}\psi_a(\mathbf{k}^2)\ ,$$

where

$$K_{na}=\int\limits_0^\infty \frac{d\mathbf{k}^2}{\pi}\psi_a(\mathbf{k}^2)\phi(\mathbf{k}^2)\ 4(\mathbf{k}^2+m^2)\psi_n(\mathbf{k}^2)\ .$$

Finally, spectral integral equation takes the form:

$$\sum_a K_{na}\psi_a(\mathbf{k}^2)-\sum_a v^{(0)}_{na}\psi_a(\mathbf{k}^2)=M_n^2\psi_n(\mathbf{k}^2)\ .$$

This is a standard homogeneous equation:

$$\sum_a s_{na}\psi_a(\mathbf{k}^2)=M_n^2\psi_n(\mathbf{k}^2)\ ,$$

with $s_{na}=K_{na}-v^{(0)T}_{na}$. The values M^2 are defined as zeros of the determinant

$$det|\hat{s}-M^2I|=0\ .$$